Intact polar lipids in the water column of the Eastern Tropical North Pacific: Abundance and structural variety of non-phosphorus lipids

Florence Schubotz [1*], Sitan Xie [1,¶], Julius S. Lipp [1], Kai-Uwe Hinrichs [1], Stuart G. Wakeham[2]

[1]MARUM and Department of Geosciences, University of Bremen, 28359 Bremen, Germany

[2]Skidaway Institute of Oceanography, Savannah, GA 31411, USA

[¶]Current address: Wai Gao Qiao Free Trade Zone, 200131 Shanghai, China

[*]Corresponding author. MARUM, University of Bremen, Leobener Str. 13, Room 1070, 28359 Bremen, Germany. Tel: +49-421-218-65724. Fax: +49-421-218-65715. E-mail: schubotz@uni-bremen.de

Keywords: intact polar lipids, phospholipids, glycolipids, betaine lipids, ether lipids, oxylipins, phospholipid substitution, oxygen minimum zone

Abstract

Intact polar lipids (IPLs) are the main building blocks of cellular membranes and contain chemotaxonomic, ecophysiologic and metabolic information, making them valuable biomarkers in microbial ecology and biogeochemistry. This study investigates IPLs in suspended particulate matter (SPM) in the water column of the Eastern Tropical North Pacific Ocean (ETNP), one of the most extensive open ocean oxygen minimum zones (OMZ) in the world with strong gradients of nutrients, temperature and redox conditions. A wide structural variety in polar lipid head group composition and core structures exists along physical and geochemical gradients within the water column, from the oxygenated photic zone to the aphotic OMZ. We use this structural diversity in IPLs to evaluate the ecology and ecophysiological adaptations that affect organisms inhabiting the water column, especially the mid-depth OMZ in the context of biogeochemical cycles. Diacylglycerol phospholipids are present at all depths, but exhibit highest relative abundance and compositional variety (including mixed acyl/ether core structures) in the upper and core OMZ where prokaryotic biomass was enriched. Surface ocean SPM is dominated by diacylglycerol glycolipids that are found in photosynthetic membranes. These and other glycolipids with varying core structures composed of ceramides and hydroxylated fatty acids are also detected with varying relative abundances in the OMZ and deep oxycline, signifying additional non-phototrophic bacterial sources for these lipids. Betaine lipids (with zero or multiple hydroxylations in the core structures) that are typically assigned to microalgae are found throughout the water column down to the deep oxycline but do not show a depth-related trend in relative abundance. Archaeal IPLs comprised of glycosidic and mixed glycosidic-phosphatidic glycerol dibiphytanyl glycerol tetraethers (GDGTs) are most abundant in the upper OMZ where nitrate maxima point to ammonium oxidation, but

43 increase in relative abundance in the core OMZ and deep oxycline. The presence of non-phosphorus
44 "substitute" lipids within the OMZ suggest that the indigenous microbes might be phosphorus limited (P
45 starved) at ambient phosphate concentrations of 1 to 3.5 μM, although specific microbial sources for many
46 of these lipids still remain unknown.

1. Introduction

Oxygen Minimum Zones (OMZ) are permanently oxygen-deficient regions in the ocean defined by O_2 concentrations <20 μM. They occur in areas where coastal or open ocean upwelling of cold, nutrient-rich waters drive elevated levels of primary production and the subsequent respiration of organic matter exported out of productive surface waters consumes oxygen faster than it is replaced by ventilation or by mid-depth lateral injections of oxygenated water. Low oxygen levels cause habitat compression, whereby species intolerant to low levels of oxygen are restricted to oxygenated surface waters (Keeling et al., 2010; Rush et al., 2012). But even these low levels of oxygen permit vertical migration of some zooplankton taxa into hypoxic waters (e.g., Seibel, 2011; Wishner et al., 2013). Oxygen depletion stimulates diverse microbial life capable of utilizing alternative electron acceptors for respiration under microaerobic conditions (e.g., Ulloa et al., 2012; Tiano et al., 2014; Carolan et al., 2015; Kalvelage et al., 2015; Duret et al., 2015). Important prokaryote-mediated processes within OMZs include denitrification and the anaerobic oxidation of ammonium (anammox), which together may account for 30-50% of the total nitrogen loss from the ocean to the atmosphere (Gruber, 2008; Lam and Kuypers, 2011). Modern day OMZs comprise ~8% of global ocean volume (Karstensen et al., 2008; Paulmier and Ruiz-Pino, 2009; Lam and Kuypers, 2011), but any expansion in the coming decades as a consequence of global warming and increased stratification (Stramma et al., 2008; Keeling et al., 2010) would have profound effects on marine ecology, oceanic productivity, global carbon and nitrogen cycles, the biological pump and sequestration of carbon (Karstensen et al., 2008; Stramma et al., 2010; Wright et al., 2012). A better understanding of the effect of low-O_2 on marine biogeochemistry and microbial ecology is thus warranted.

The Eastern Tropical North Pacific Ocean (ETNP), situated off the west coast of Mexico and Central America, hosts one of the largest OMZs in the open ocean, extending halfway across the Pacific Ocean and comprising ~41% of global OMZs (Lavín and Fiedler, 2006; Fiedler and Talley, 2006; Paulmier and Ruiz-Pino, 2009). By comparison, OMZs of the Eastern Tropical South Pacific Ocean off Peru and Chile and in the Arabian Sea are ~14% and ~8%, respectively, of global OMZs. In the ETNP, a sharp permanent pycnocline develops where warm, saline surface waters lie on top of a shallow thermocline, producing a highly stratified water column. Moderate primary production, dominated by picoplankton, depends on oceanic upwelling and wind mixing of coastal waters but is generally limited by the lack of micronutrient dissolved iron (Franck et al., 2005; Pennington et al., 2006). Remineralization, ~70% of which is microbially mediated (Cavan et al., 2017), of particulate organic carbon exported out of surface waters consumes oxygen at rates that cannot be balanced by ventilation across the pycnocline and by sluggish lateral circulation, leading to O_2 levels <2 μM at depths between ~100 and ~800 m. Abundances of micro- (Olson and Daly, 2013) and macro-zooplankton (Wishner et al., 2013; Williams et al., 2014) that are high in surface waters are reduced in the OMZ, and those macrozooplankton that are diel vertical migrators survive in the OMZ with reduced metabolic rates (Maas et al., 2014; Cass and Daly, 2015). Microbial abundances and activities for both heterotrophic and chemoautotrophic metabolisms are high in both surface waters and within the OMZ, but again with reduced metabolic rates in the OMZ (Podlaska et al., 2012). A strong nutricline indicates microbial nitrogen cycling involving co-occurring nitrification, denitrification and anammox (Rush et al., 2012; Podlaska et al., 2012), perhaps contributing up to 45% of the global pelagic denitrification (Codispoti and Richards, 1976). Microbial communities are mainly comprised of proteobacteria, with increasing contributions of archaea in deeper waters. Yet, on

88 average ca. 50% of the prokaryotic communities within the OMZ of the ETNP remained uncharacterized
89 (Podlaska et al., 2012).

90 Intact polar lipids (IPLs) are the main building blocks of cellular membranes and may be used to
91 characterize abundance and physiology of aquatic microorganisms from all three domains of life. IPLs
92 represent a diverse range of molecular structures, including phosphatidyl, glycosidic, phospho-glycosidic,
93 and amino acid polar head groups linked to glyceryl-acyl and glyceryl-*O*-alkyl apolar moieties. IPL
94 distributions have been documented in surface waters of the Eastern Subtropical South Pacific (Van Mooy
95 and Fredricks, 2010), the Western North Atlantic Ocean (Van Mooy et al., 2006; 200; Popendorf et al.,
96 2011a), the South Pacific Ocean (Kharbush et al., 2016), the Mediterranean Sea (Popendorf, et al., 2011b),
97 the North Sea (Brandsma et al., 2012), lakes (Bale et al., 2016), the Western English Channel (White et
98 al., 2015) and throughout the water columns of stratified water bodies (Ertefai et al., 2008; Schubotz et
99 al., 2009; Wakeham et al., 2012; Pitcher et al., 2011; Xie et l., 2014; Basse et al., 2014; Sollai et al., 2015).
100 Surface waters are typically dominated by nine IPL classes. Three diacylglycerol glycolipids,
101 monoglycosyl (1G-), diglycosyl (2G-) and sulfoquinovosyl diacylglycerol (SQ-DAG), are main IPLs
102 found in all thylakoid membranes of phototrophs, including those of cyanobacteria (Siegenthaler et al.,
103 1998)[1]. Three betaine lipids, diacylglyceryl homoserine (DGTS), hydroxymethyl-trimethyl-*β*-alanine
104 (DGTA) and carboxy-*N*-hydroxymethyl-choline (DGCC), are also generally abundant. Betaine lipids
105 are widely distributed in lower plants and green algae (Dembitsky, 1996) and are thus usually assigned to

[1] Elsewhere in the literature 1G-DAG, 2G-DAG, and SQ-DAG are also termed MGDG, DGDG and SQDG. However, we have opted to retain the 1G-DAG, 2-DAG, etc. nomenclature as other IPLs discussed throughout also contain monoglycosyl- and diglycosyl-moieties (e.g., 1G-GDGT and 2G-GDGT). Likewise, we retain the nomenclature PC-DAG, PE-DAG, and PG-DAG for phospholipids elsewhere termed PC, PE, PG.

106 eukaryotic algae in the ocean (Popendorf, et al., 2011a), but DGTS was recently also found in bacteria
107 when phosphorus is limited (Yao et al., 2015; Sebastian et al. 2016). Three common detected
108 phospholipids are diacylglycerol phosphatidyl choline (PC-DAG; often simply referred to elsewhere as
109 PC), phosphatidyl ethanolamine (PE-DAG, often PE), and phosphatidyl glycerol (PG-DAG, often PG),
110 all of which have mixed eukaryotic or bacterial sources in the upper water column (Sohlenkamp et al.,
111 2003; Popendorf, et al., 2011a). Microbial source assignments have been broadly confirmed by isotope
112 labeling studies (Popendorf, et al., 2011a). In oxygen-deficient subsurface waters IPL distributions are
113 more diverse and other phospholipids such as diacylglycerol phosphatidyl (*N*)-methylethanolamine
114 (PME-DAG), phosphatidyl (*N,N*)-dimethylethanolamine (PDME-DAG) and diphosphatidyl glycerol
115 (DPG) increase in abundance; these IPLs occur in a number of bacteria that may inhabit low oxygen
116 environments (Schubotz et al., 2009; Wakeham et al., 2012). Dietherglycerol phospholipids and
117 glycosidic ceramides with unidentified sources have also been detected (Schubotz et al., 2009; Wakeham
118 et al., 2012), the latter have been recently observed to be abundant in phosphorus-limited diatoms (Hunter
119 et al., 2018). IPLs that are unique to marine archaea are comprised of glycerol dialkyl glycerol tetraethers
120 (GDGT) core lipids with various glycosidic, diglycosidic and mixed phospho-glyco polar head groups
121 (e.g., Schouten et al., 2008; Pitcher et al., 2011; Zhu et al., 2016; Elling et al., 2017). Abundances of
122 archaeal IP-GDGTs vary considerably with depth, but are typically elevated in zones of water column
123 oxygen depletion, especially where ammonium oxidizing thaumarchaea are abundant (Pitcher et al., 2011;
124 Schouten et al., 2012; Sollai et al., 2015).

125 IPL can also be indicators of metabolic and physiologic status. Many organisms remodel their IPL
126 composition when faced with environmental stressors such as changes in pH, salinity, temperature or

127 availability of nutrients (Zhang and Rock, 2008; Van Mooy et al., 2009; Meador et al., 2014; Carini et al.,
128 2015; Elling et al., 2015). Replacing phospholipids with non-phosphorus containing substitute lipids is
129 an important mechanism when facing nutrient phosphate starvation in oligotrophic surface waters where
130 phosphate concentrations may be as low as nanomolar levels. Cyanobacteria replace PG-DAG with SQ-
131 DAG (Benning et al., 1993; Van Mooy et al., 2006) and microalgae and some bacteria replace PC-DAG
132 with DGTS (Geiger et al., 1999; Van Mooy et al., 2009; Popendorf, et al., 2011b) due to their similar ionic
133 charge at physiological pH. Heterotrophic marine bacteria can replace PE-DAG with either 1G-DAG or
134 DGTS (Carini et al., 2015; Sebastian et al., 2016; Yao et al., 2015). Notably, substitute lipids are also
135 biosynthesized under micromolar concentrations of phosphate (Bosak et al., 2016).

136 Here, we use IPL distributions in suspended particulate matter (SPM) to characterize eukaryotic,
137 bacterial and archaeal communities inhabiting the water column of the ETNP. This study is an extension
138 of that of Xie et al. (2014), which focused on the distribution of core and intact polar archaeal and bacterial
139 tetraether lipids at two stations investigated here (stations 1 and 8). The water column of the ETNP
140 comprises distinct biogeochemical zones based on oxygen concentrations and IPL distributions reflect the
141 localized ecology. Abundant non-phosphorus substitute lipids within the core of the OMZ suggest
142 phosphorus limitation of the source microorganisms even at micromolar concentrations of phosphate.
143 Overall our results provide deeper insight into the broad community composition and the physiologic state
144 of microorganisms inhabiting OMZs.

145

146 **2. Methods**

147 *2.1 Sample collection and CTD data*

148 Suspended particulate matter (SPM) samples were collected at four stations (distance to shore:
149 400~600 km; Fig 1) along a northwest-southeast transect (Station 1: 13° 01.87'N，104° 99.83'W; Station
150 2: 11° 99.96' N，101° 22.82' W; Station 5: 10° 68.94' N，96° 34.12' W; and Station 8: 8° 99.46'N，
151 90°00.18'W) in the ETNP during the R/V *Seward Johnson* cruise in November 2007 (R/V *Seward Johnson*
152 Cruise Scientists, 2007). Station 1 in the Tehuantepec Bowl is an area of relatively low primary
153 productivity (e.g., 0.05 mg Chl-*a*/m^2; (Fiedler and Talley, 2006; Pennington et al., 2006) whereas Station
154 8 in the Costa Rica Dome is moderately productive (1 mg Chl-*a*/m^2). All stations are characterized by a
155 strong thermocline/pycnocline/oxycline (at 20-50 m depths depending on location) and a profound and
156 thick OMZ (down to ~2 μM O_2 between ~300-800 m depth). Station 1 is a reoccupation of the Vertical
157 Transport and Exchange II/III site from the early 1980's (Lee and Cronin, 1984; Martin et al., 1987;
158 Wakeham and Canuel, 1988; Wakeham, 1987, 1989).

159 Seawater was filtered *in-situ* using submersible pumps (McLane Research Laboratories WTS-142
160 filtration systems) deployed on the conducting cable of the CTD/rosette that measured temperature,
161 conductivity, oxygen, fluorescence/chlorophyll-*a* and transmissivity during pump deployments and
162 during pumping. Filtered water volumes ranged between 130 and 1800 L (Suppl. Table 1). Pumps
163 were fitted with two-tier 142 mm diameter filter holders: a 53 μm mesh Nitex "prefiltration" screen to
164 remove larger eukaryotes and marine snow aggregates and a double-stacked tier of ashed glass fiber filters
165 (142 mm Gelman type A/E, nominal pore size 0.7 μm). IPL concentrations we report represent minimum
166 values to reflect potentially inefficient collection of 0.7 μm particles by GFFs. Since pore size of the
167 filters may also decrease during filtration the recovered material may vary dependent on filtration time.

168 Following pump recovery, GFF filters and Nitex screens were wrapped in pre-combusted foil and stored
169 frozen at -20°C until extraction.
170
171 *2.2 Elemental, pigment and nutrient analysis*
172 Particulate organic carbon (POC) and total particulate nitrogen (TN) were measured on 14 mm-
173 diameter subsamples of each glass fiber filter (GFF) prior to lipid extraction; therefore, POC and TN
174 concentrations reported here are only for <53 μm material. The plugs were acidified in HCl vapor in a
175 desiccator for 12 hours to remove inorganic carbon. Elemental analysis was performed with a
176 ThermoFinnigan Flash EA Series 1112 interfaced to a ThermoFinnigan Delta V isotope ratio mass
177 spectrometer at the Skidaway Institute Scientific Stable Isotope Laboratory. Organic carbon and
178 nitrogen contents were calibrated against internal laboratory chitin powder standards which in turn had
179 previously been cross-calibrated against USGS 40 and 41 international standards.
180 Chlorophyll-*a* (Chl-*a*) and pheopigment concentrations were measured on-board the ship (Olson and
181 Daly, 2013). Seawater samples (100 – 500 ml) from CTD casts were filtered onto Whatman GF/F filters
182 (0.7 μm) which were immediately extracted with 90% acetone. Fluorescence was measured with a
183 Turner Designs 10AU fluorometer and Chl-*a* concentrations were determined after Parsons et al (1984).
184 Post-cruise HPLC analysis of pigments in 100 − 500 ml seawater samples filtered onto Whatman GF/F
185 (0.7 μm) filters were conducted at the College of Charleston Grice Marine Laboratory, Charleston, SC on
186 a Hewlett Packard 1050 system (DiTullio and Geesey, 2002).
187 Seawater samples for nutrient analyses (NO_2^-, NO_3^{-2}, NH_4^+ and PO_4^{3-}) were collected directly from
188 Niskin bottles into acid-washed, 30-mL high-density polyethylene (HDP) bottles. After three rinses,

189 bottles were filled to the shoulder, sealed, and frozen (−20°C). All frozen samples were transported to
190 the Oceanic Nutrient Laboratory at USF for analysis using a Technicon Autoanalyzer II.
191
192 *2.3 Lipid extraction and analysis of intact polar lipids*
193 Lipids associated with the <53 μm SPM on the GFFs were Soxhlet-extracted shortly after the
194 expedition in 2008 using dichloromethane:methanol (DCM:MeOH; 9:1 v/v) for 8 h. Extracted lipids
195 were partitioned into DCM against 5% NaCl solution and dried over Na_2SO_4. Total lipid extracts (TLEs)
196 were stored at -20°C. Soxhlet extractions, rather than for example microwave assisted Bligh-Dyer
197 extractions, were chosen at the time because it was the only feasible way to handle the double 142mm
198 filters. Extraction protocol surely can affect IPL distributions; as shown by Lengger et al. (2012) for
199 smaller sediment samples.
200 IPL analyses by high-performance liquid chromatography-mass spectrometry (HPLC-MS) were
201 carried out initially in 2010/2011 and again in 2015 as instrument protocols improved. In between these
202 analyses we did not observe a notable selective loss of IPL compounds, instead we were able to detect a
203 much larger suite of IPL structures due to improved detection and chromatographic separation techniques
204 (Wörmer et al., 2013). The confidence in these results are supported by the analysis of IPL standards
205 (Suppl. Table 2) that are stored at -20 °C over several years (fresh standard mixtures are typically prepared
206 every 2 to 3 years), which do not indicate degradation of any particular IPL over time (Suppl. Fig. 1).
207 The analyses in 2010/2011 focused on determining absolute concentrations of the major IPLs (for
208 distinction between major and minor IPLs see results section). Aliquots of the TLE were dissolved in
209 DCM/methanol (5:1 v/v) for injection on a ThermoFinnigan Surveyor HPLC system coupled to a

210 ThermoFinnigan LCQ DecaXP Plus ion-trap MS via electrospray interface (HPLC-ESI-IT-MS^n) using
211 conditions described previously (Sturt et al., 2004; Xie et al., 2014). Ten µL of a known TLE aliquot
212 spiked with C_{19}-PC as internal standard was injected onto a LiChrosphere Diol-100 column (150 × 2.1
213 mm, 5 µm, Alltech, Germany) equipped with a guard column of the same packing material. Absolute
214 IPL concentrations were determined in positive ionization mode with automated data-dependent
215 fragmentation of the two most abundant base peak ions. Acyl moieties of glycolipids and aminolipids
216 were identified via HPLC-IT-ESI-MS^2 experiments in positive ionization mode, whereas phospholipid
217 side chain composition was analyzed in negative ionization mode. Details of mass spectral interpretation,
218 and identification of fatty acid moieties are described in Sturt et al. (2004) and Schubotz et al. (2009) and
219 are exemplified in Suppl. Table 3. HPLC-MS analysis is not able to differentiate between double bonds
220 or rings, therefore in the subsequent text we will refer to double bond equivalents (DBE) to include both
221 possibilities, similarly absolute chain length cannot be determined as branched and straight chain alkyl
222 chains cannot be differentiated, therefore we report total carbon atom numbers for the alkyl side chains.
223 Assignment of the betaine lipid DGTS was according to the retention time of the commercially available
224 standard DGTS (Avanti Polar Lipids, USA). The isomer DGTA, which elutes at a different retention
225 time due to its structural difference (e.g., Brandsma et al., 2012) was not observed in the HPLC-MS
226 chromatograms. For all analyses, response factors of individual IPLs relative to the injection standard
227 C_{19}-PC were determined using dilution series of commercially available standards (Suppl. Table 2).

228 Subsequent analyses in 2015 were used to obtain sum formulas and IPL structures based on exact
229 masses in the MS1 and MS-MS experiments and to additionally provide data on minor lipids, which were
230 below detection limit during the 2010/2011 ion trap analyses (for distinction between major and minor

231 lipids see results section). For the 2015 measurements absolute quantities could not be determined since
232 the TLE had been used for other experiments and the information on TLE amounts used was unknown;
233 therefore, these analyses are used to describe relative abundances. Analyses were performed on a Bruker
234 maXis Plus ultra-high resolution quadrupole time-of-flight mass spectrometer (Q-TOF) with an ESI
235 source coupled to a Dionex Ultimate 3000RS UHPLC. Separation of IPLs was achieved using a Waters
236 Acquity UPLC BEH Amide column as described in Wörmer et al. (2013), which resulted in better
237 chromatographic separation of compounds and higher sensitivity compared to the 2010/2011 analyses.
238 Peak areas in extracted mass chromatograms were corrected with absolute response factors determined in
239 dilution series of commercially available standards (Suppl. Table 2). Some ions assigned to either PE-
240 AEG and PC-AEG could not be quantified individually due to co-elution of these compounds and were
241 thus quantified as one group using the mean response factor of PE- and PC-DAG. For compound classes
242 for which no standards were available, (e.g., PI-DAG, OL and the unknown aminolipids AL-I and AL-II)
243 the relative responses could not be corrected for. Assuming these compounds may ionize similarly as
244 structurally related IPLs, values may be off by a factor of 0.2 to 1.4, which is the maximum range of
245 response factors observed for the standards.
246
247 *2.4 Statistical analysis*
248 Nonmetric multidimensional scaling (NMDS) analysis was used to illustrate the relationships
249 among objects hidden in a complex data matrix (Rabinowitz, 1975) and was performed in the free software
250 R (version 3.4.3, www.r-project.org/) with *metaMDS* (vegan library, version 2.4-6) as described by
251 Wakeham et al. (2012). The datasets of relative lipid distribution and variations in carbon number and

252 double bond equivalents were standardized by Hellinger transformation using the function *decostand*,
253 while for all other variables (environmental parameters, microbial groups) absolute numbers were used.
254 The compositional dissimilarity was calculated by Euclidean distance measure. The resulting plot shows
255 the distribution of lipids and sampling depths. Microbial groups and geochemical parameters were
256 overlaid by function *envfit*. Lower stress is related to high quality of solution, and stress values ≤ 0.1
257 indicate results of good quality (Rabinowitz, 1975). Non-parametric Spearman Rank Order Correlation
258 analysis was performed on combined data of environmental variables and IPL ratios and IPL relative
259 abundances of all four stations using SigmaPlot 11.0 (Systat Software Inc., San Jose, USA).
260
261 **3. Results**
262 *3.1 Biogeochemical setting*
263 All along the transect, the thin mixed layer (upper ~20 m) was warm, ~25−28 °C, with oxygen
264 concentrations approaching air saturation at ~200 μM (Fig. 2). The euphotic zone (1% of surface
265 photosynthetically active radiation) generally ranged between 50 and 80 m depth. The thermocline was
266 abrupt at ~20-50 m, where temperatures dropped to ~15−18 °C and oxygen decreased to ~20 μM.
267 Temperatures stabilized by ~250−300 m depth at ~10−12 °C and oxygen levels were <2 μM; especially
268 at Station 8 there were spatially and temporally variable oxygen intrusions into the upper portion of the
269 OMZ. By ~600−800 m depth, a deep oxycline was observed where oxygen concentrations began to rise
270 again to ~40 μM at temperatures of ~4 °C by 1250 m. For the purposes of this discussion, the water
271 column of the ETNP was partitioned into four horizons based on oxygen content: an oxic epipelagic zone
272 down to the thermocline (0–50 m; 200 μM > O_2 > 20 μM); an upper OMZ (Station 1 and 8: 50–300 m,

Station 5: 50 – 350 m, Station 2: 50–200 m; 20 μM > O_2 > 2 μM); the core OMZ (Station 1 and 8: 300–800 m, Station 5: 350 – 600 m Station 2: 200 – 600 m; O_2 < 2 μM); and a deep oxycline (Station 1 and 8 ≥ 800 m, Station 2 and 5 ≥ 600 m; O_2 > 2 μM) of rising O_2 levels (Fig. 1a). Note that sampling at stations 1 and 8 reached to 1250 m depth so SPM from >750 m depth best represents the deep oxycline.

Chl-*α* was highest in surface waters with maximum values of 1.8 μg/L at 10 m at station 5, was between 0.2 and 0.7 μg/L at station 1, 2 and 8 and decreased to values close to zero below 100 m at all stations (Fig. 2; see also Fiedler and Talley, 2006, and Pennington et al., 2006, for additional results from previous surveys). HPLC analysis of accessory pigments (Goericke et al., 2000; Ma et al., 2009) showed that picoplankton, primarily *Prochlorococcus* (indicated by divinyl chlorophyll *α*), were an important component of the photoautotrophic community, along with diatoms (fucoxanthin), especially *Rhizosolenia* at the deep fluorescence maximum at stations 1 and 5 but *Chaetoceros* at station 8, and prymnesiophytes (19'hexanoyloxyfucoxanthin and 19'butanoyloxyfucoxanthin; DiTullio and Geesey, 2002; Suppl. Table 4). High phaeopigment abundances (up to 90% of [Chl-*α* + phaeopigments]) attested to algal senescence or grazing by macro- (Wishner et al., 2013; Williams et al. 2014) and micro-zooplankton (Olson and Daly, 2013) above and into the oxycline. Primary maxima in transmissivity corresponded with the peak Chl-*α* concentrations and fluorescence maxima, but secondary transmissivity maxima between 300 and 400 m at stations 1, 5, and 8 indicated elevated particle abundances in the core of the OMZ (Fig. 2).

Nitrite (NO_2^-) maxima in the OMZ at all stations coincided with nitrate (NO_3^{2-}) deficits (Fig. 3). Ammonium (NH_4^+) concentrations changed little through the water column (Fig. 3). Phosphate (PO_4^{3-}; Fig. 3) and total dissolved nitrogen (TDN; not shown) were low (respectively, < 0.5 and < 3 μM) in the upper 20 m of the oxic zone, but increased in the OMZ. High PO_4^{3-} (up to 3.4 μM) and high TDN (up

294 to 44.5 μM) were observed in the deep OMZ at stations 2, 5 and 8 (Fig. 3). N:P ratios were lower than
295 the Redfield ratio (16) at all sites and depths (Fig. 3); N:P minima were lowest in surface waters (2.6 to
296 10 in the upper 20 m) and at ~500 m within the core OMZ and the deep oxycline at station 1 (<9).
297 POC and TN concentrations (< 53 μm material) were highest in the euphotic zone (POC: 20 – 100
298 μg/L; TN: 4 – 15 μg/L), rapidly dropping to 5 μg/L and 1 μg/L below the upper OMZ, respectively (Fig.
299 2; Suppl. Fig. 2). Secondary maxima for POC (~10 μg/L) and TN (~2 μg/L) within the core of the OMZ
300 might reflect elevated microbial biomass there. Concentrations dropped in the deep oxycline to ≤3 μg/L
301 and ≤0.5 μg/L for POC and TN, respectively.
302 Absolute IPL concentrations were determined by ion trap LCMS and varied between 250 and 1500
303 ng/L in the oxic zone and abruptly decreased more than 10-fold (to <20 ng/L) in the upper OMZ (Fig. 2).
304 Secondary maxima in IPL concentrations (15–40 ng/L) within the OMZ at all stations roughly coincided
305 with elevated numbers of prokaryotes (Fig. 2). IPL:POC ratios decreased with increasing depth (Fig. 2),
306 tracking trends of POC, TN and IPL concentrations.
307
308 *3.2 Changes in IPL composition with water column depth in the ETNP*
309 In total, 24 IPL classes were identified in the ETNP (Fig. 4, Suppl. Fig. 3). Eleven major and thirteen
310 minor IPL classes were detected in the QTOF analyses, which were classified according to their relative
311 abundance: if an individual IPL comprised more than 10% of total IPLs at any depth of the four stations
312 it was classified as a major IPL, compounds <10% were minor IPLs. Based on their head group
313 composition IPLs were grouped into glycolipids, phospholipids or aminolipids. Figure 3 shows changes
314 in the relative abundances (as percentages of total IPLs, excluding isoprenoidal archaeal IPLs) of

glycolipids, phospholipids and aminolipids as well as several substitute lipid ratios, reflecting preferential biosynthesis of non-phosphorus lipids to replace phospholipids under phosphate-limiting growth (cf. Van Mooy et al., 2006; Popendorf, et al., 2011b; Carini et al., 2015; Bosak et al., 2016). Relative abundances of non-isoprenoidal phospholipids were highest in the core OMZ between 400 and 600 m at all sites, where they comprise up to 45−76% at stations 1, 2 and 5 and between 12 and 61% at station 8. Phospholipid abundances were lower within the upper OMZ and oxic zone at all stations (between 4 and 55%) and in the deep oxycline at station 8 (<1%). Aminolipid content was highest in SPM from the upper 55 m at station 5 and 8 (10 to 25%), the core OMZ at station 8 (15 to 34%) and the deep oxycline at station 1 (17%). Lower aminolipid contents (2 to 11%) were observed in the oxic zone and the core OMZ at stations 1 and 2, the upper OMZ at station 5 (0 to 11%) and the deep oxycline at station 8 (<2%). Glycolipid abundance was >9% at all depths, with highest abundance (average 54%, max. 82%) within the upper OMZ and oxic zone at all stations and the deep oxycline at station 8. Values down to 9% were observed within the core OMZ.

3.2.1 Major lipids

The eleven major IPL classes included three IP-GDTs of archaeal origin: (1G-GDGT, 2G-GDGT and HPH-GDGT); and eight IPLs assigned to either a bacterial or eukaryotic origin: three glycolipids (1G-DAG, 2G-DAG, SQ-DAG), four phospholipids (PG-DAG, PE-DAG, PC-DAG, PE+PC-AEG) and one aminolipid (DGTS). All major lipid classes were found at almost all depths at all four stations, but with varying relative abundances (as % of total IPL; Fig. 4, Suppl. Table 1).

Archaeal IP-GDGTs: Relative abundances of archaeal IPL (IP-GDGTs) generally increased with

depth from non-detectable in surface waters to >50% of total IPLs at station 8 (bottom of core OMZ and deep oxycline). Archaeal IP-GDGT abundances at stations 1 and 2 peaked at 30% (bottom of upper OMZ, core OMZ and deep oxycline) but were generally <10% at station 5 (Fig. 4). At station 1 and 2, 1G-GDGT and 2G-GDGT were most abundant with variable amounts of HPH-GDGTs, whereas 1G-GDGT and HPH-GDGT dominated archaeal IPLs at station 5 and 8 at most depths. Distributions of glycosidic IPL-GDGTs obtained in the present investigation corroborate the absolute values reported by (Xie et al., 2014) for stations 1 and 8: 1G-GDGT was more abundant than 2G-GDGT at station 8 when compared to station 1. The core GDGTs of 1G-GDGTs and HPH-GDGTs are dominated by GDGT-0 and crenarchaeol (Suppl. Fig. 4), whereas 2G-GDGTs are dominated by GDGT-2 and a small amount of crenarchaeol (Zhu et al., 2016)

Diacylglycerol lipids: The oxic zone and the upper OMZ were dominated (~50−80% of IPL) at all sites by the diacylglycerol glycolipids, 1G-DAG, 2G-DAG and SQ-DAG (Fig. 4). In the core OMZ and deep oxycline, relative amounts of 2G-DAG and SQ-DAG decreased to 4% and 12%, respectively. 1G-DAG abundances were lowest in the core OMZ at all stations, but were up to 47% of total IPL in the deep oxycline. Diacylglycerol phospholipids, PE-, PG- and PC-DAG, were the second most abundant IPLs. Abundances of PE- and PG-DAG were highest within the upper and core OMZ, constituting >50% in the core OMZ at station 1, >30% at stations 2 and 5, and 16% at station 8. PC-DAG, with average abundances of 5% at stations 1, 2, 8 and 3% at station 5, did not exhibit depth-related trends. The third most abundant diacylglycerol class was the betaine lipid DGTS, which was present throughout the water column at average abundances of 7% at station 1, 2 and 8, and 5% at station 5.

Major diacylglycerol lipids showed changes in average number of carbon atoms and double bond

357 equivalents (DBE) with depth (Fig. 5, Suppl. Table 5). The glycolipids and PC-DAG decreased in average
358 carbon number by up to three carbons and decreased in DBE by up to 2 at the top of the upper OMZ and
359 within the core OMZ compared to the oxic zone and the deep oxycline. Average carbon numbers for
360 PE- and PG-DAG and DGTS showed an inverse trend, both generally increasing up to two carbons
361 between the upper OMZ and the core OMZ. Changes in DBE were not as pronounced for PG-DAG and
362 DGTS, on average 1 to 2 DBE greater in surface waters than in deeper waters, while the number of DBE
363 increased on average with depth for PE-DAG.

364 *Acyl-ether glycerol lipids*: Mixed ether-ester glycerol core structures with either PE or PC head
365 groups were observed at all stations and all depths (generally 4-12%) except for the deep oxycline at
366 station 8.

367

368 *3.2.2 Minor lipids*

369 Thirteen minor IPL classes were identified, five of which were glycolipids, four phospholipids and
370 four aminolipids. All minor lipid classes were detected at each site except for OH-DGTS which was
371 absent at station 1. Some minor lipids were found at all depths, whereas others were restricted to specific
372 depth zones as defined by oxygen content (Fig. 4).

373 *Diacylglycerol lipids:* Two minor diacylglycerol glycolipids, 1G-OH-DAG and 3G-DAG, were
374 most abundant within the oxic zone and the upper OMZ, comprising between 2 to 15% of minor lipids on
375 average (0.1 to 0.6% of total IPLs), but were only sporadically found within the core OMZ and deep
376 oxycline. 1G-OH-DAG showed highest relative abundances at station 5, constituting up to 40% of minor
377 lipids. Four additional phospholipids with diacylglycerol core structures with the following head groups

were identified: diphosphatidylglycerol (DPG), phosphatidyl-(*N*)-methylethanolamine (PME), phosphatidyl-(*N,N*)-dimethylethanolamine (PDME) and phosphatidyl inositol (PI). DPG, PME-DAG and PDME-DAG had highest relative abundances (respectively 65, 56 and 35% of minor IPL) within the upper and core OMZ, but at lower abundances within the oxic zone at all stations and in the deep oxycline at stations 1, 2 and 5. PI-DAG was most abundant in the oxic zone and the upper OMZ (up to 25% of minor IPL), but was also present in the core OMZ and the deep oxycline, except for station 8. Three types of aminolipids were observed as minor lipids. OH-DGTS with up to three hydroxyl-groups attached to the fatty acyl side chains (Suppl. Fig. 5) was observed at most depths at station 8 with an average relative abundance of 23% among the minor lipids; it was also occasionally detected at stations 2 and 5 within the oxic zone and upper OMZ. Two additional aminolipids had an undefined head group that exhibited fragmentation patterns characteristic of betaine lipids, but without established betaine head group fragments (Suppl. Fig. 6b, c). The tentatively assigned sum formula for the head group of the first unknown aminolipid (AL-I) at ca. 6.7 minutes LC retention time was $C_8H_{17}NO_3$ and for the second unknown aminolipid (AL-II) at 10.5 minutes was $C_7H_{15}NO_3$. The head group sum formula for AL-II matches that of DGCC, but the diagnostic head group fragment of m/z 252 was not detected, and furthermore, AL-II did not elute at the expected earlier retention time for DGCC. AL-I and AL-II were detected at most depths at all four stations, with average abundances of 1 to 6% of the minor lipids for AL-I and comparably higher relative abundances ranging from 16 to 36% for AL-II.

Acyl-ether glycerol lipid: One minor compound that eluted slightly earlier than SQ-DAG had a fragmentation pattern similar to SQ-DAG but with exact masses of the parent ion and MS-MS fragments in both positive and negative ion mode that suggested a mixed acyl-ether glycerol core lipid structure

(Suppl. Fig. 6 d, e). Tentatively assigned as SQ-AEG, this IPL was observed at most depths at all four stations with highest relative abundances of 5 to 60% of minor IPLs within the oxic zone.

Sphingolipids: Two types of sphingolipids were identified, monoglycosyl ceramide (1G-CER), and hydroxylated monoglycosyl ceramide (1G-OH-CER) with up to two hydroxyl groups attached to the hydrophobic side chains (Suppl Fig. 5e). Both were observed at all depths at stations 1, 2, and 5 at average relative abundances between 3 and 8% of minor IPLs, but neither was detected in the deeper part of the core OMZ or deep oxycline at station 8.

Ornithine lipids: Trace amounts (<4%) of ornithine lipids were detected in the core OMZ of stations 2 and 5.

3.2.3 Statistical relationships between environmental parameters and lipid distribution

Spearman Rank Order Correlation was used to evaluate relationships between relative lipid abundance of lipid classes and environmental parameters (Table 1). The glycolipids 2G- and SQ-DAG showed highly significant ($p<0.001$) and positive correlations with depth, fluorescence, POC, TN, temperature and Chl-α, significant positive correlations were also observed with oxygen. Both also showed highly significant but negative correlations with phosphate and nitrate, and these overall trends were mirrored in the SQ-DAG:PG-DAG ratio. Total glycolipids (GL) and 1G-DAG only showed correlations with a few environmental parameters and total GL were only significantly positively correlated with oxygen. Most aminolipids and phospholipids did not show significant correlations with environmental parameters and any other correlations were neither strongly positive nor negative. Relative abundances of total aminolipids and aminolipid (AL) to phospholipid (PL) ratios correlated

positively with ammonium. AL:PL also correlated positively with oxygen. Relative abundance of total phospholipids and most individual phospholipids (PG-, PE-, PME-, and PDME-DAG) correlated negatively with oxygen. The only phospholipid that significantly correlated with phosphate was PDME, however, the positive correlation is not strong (r^2<0.4).

NMDS analysis revealed that all samples from the oxic zone had a negative loading on the NMDS2 axis along with environmental variables such as oxygen, fluorescence, TN, POC and Chl-*α*. IPLs with a strong negative loading on the NMDS2 axis (<-0.2) were 1G-OH-DAG, SQ-AEG, 2G-DAG, SQ-DAG, PI-DAG and OH-DGTS. Most samples from the core OMZ and deep oxycline had a positive loading on the NMDS2 axis, together with depth, phosphate and nitrate. IPLs that showed a strong positive loading on the NMDS2 axis (>0.2) were PDME-DAG, 2G-GDGT, DPG, PME-DAG and HPH-GDGT. Almost all environmental variables had low *p*-values (<0.001), indicating highly significant fitted vectors with the exception of temperature, salinity, ammonium and nitrate. Highest goodness of fit statistic was observed with oxygen (r^2=0.54), followed by phosphate (r^2=0.48) and then fluorescence (r^2=0.46).

4. Discussion

The moderate primary productivity in surface waters of the ETNP, intense microbial degradation of particulate organic matter exported to the thermocline, and restricted midwater oxygen replenishment produce the strong, shallow (~20 m deep) oxycline and a ~500 m thick OMZ with dissolved oxygen concentrations of <2 μM, not unlike other oceanic OMZs (e.g., Ulloa et al., 2012). The ETNP is dominated by picoplankton, and micro-grazers reported consuming most phytoplankton production (Landry et al., 2011; Olsen and Daly, 2013). Peak macrozooplankton biomass was located at the

441 thermocline, near the upper boundary of the OMZ, but a secondary biomass peak of a different
442 zooplankton assemblage was present at the deep oxycline once O_2 concentrations rose to ~2 μM (Wishner
443 et al., 2013). Shallow-water, plankton-derived particulate organic carbon is the primary food source for
444 zooplankton in the mixed layer, upper oxycline and core OMZ, whereas deep POC, some of which might
445 have been produced by microbes in the OMZ, is important for deep oxycline zooplankton (Williams et al.,
446 2014). Microbial community structure and activities are typical of other OMZs (Taylor et al., 2001; Lin
447 et al., 2006; Woebken et al., 2007; Wakeham et al., 2007; 2012). Cell numbers of total prokaryotes were
448 highest in the euphotic layer and decreased with depth at the thermocline but rose again within the core
449 OMZ (Podlaska et al., 2012). Elevated rates of chemoautotrophy, measured by dark dissolved inorganic
450 carbon (DIC) assimilation, were observed at several depths in the OMZ and in the lower oxycline.
451 Transfer of chemoautotrophically-fixed carbon into zooplankton food webs is also evident (Williams et
452 al., 2014). Bacteria dominate the prokaryotic community at all stations. Nitrifying bacteria constituted
453 3-7% of total DAPI-positive prokaryotes in surface waters; sulfate-reducing bacteria (17 and 34% of total
454 prokaryotes), planctomycetes (up to 24% of total prokaryotes), and anammox bacteria (<1% of
455 prokaryotes) in the upper OMZ and deep oxycline might be associated with anoxic microzones within
456 particle aggregates even at low dissolved oxygen concentrations (Woebken et al., 2007; Carolan et al.,
457 2015). Archaeal cell abundances peaked at the start of the upper OMZ at all stations (up to 37% of total
458 prokaryotes at station 2), within the core OMZ at station 2 (up to 54% of total detected cells) and within
459 the deep oxycline at station 5 and 8 (around 25%; Fig. 2e). Crenarchaeota/thaumarchaeota represented
460 ~20% of prokaryotes throughout the water column, generally being highest in the lower OMZ and deep
461 oxycline, and at stations 2 and 5 just above the secondary Chl-*a* maxima at ~75 m. Euryarchaeota were

16-20% of total prokaryotes, especially in waters above the OMZ.

Total IPL concentrations that were over 50 times higher in the surface waters than at deeper depths coincided with high Chl-α concentrations, reflecting the importance of phototrophic sources to the IPL pool above the thermocline. Below the thermocline, IPL concentrations generally track trends in microbial cell abundances, and elevated IPL concentrations in the upper and core OMZ coincide with elevated nitrite concentrations. The rapid decrease in IPL concentrations below ~100 m probably results from a combination of a dearth of potential source organisms and the decomposition of sinking detrital lipids (Harvey et al., 1986; Matos and Pham-Thi, 2009). IPL concentration decreases below the euphotic zone are well established (Van Mooy et al., 2006; Schubotz et al., 2009; Van Mooy and Fredricks, 2010; Popendorf et al., 2011b; Wakeham et al., 2012). We believe that the diverse molecular compositions and shifts in relative abundances of IPLs with changing geochemistry reflect a complex biological community structure and their ecophysiologic adaptation throughout the water column.

4.1 Provenance of IPLs in the ETNP

Variations in IPL distributions and head group and core lipid compositions reflect the biogeochemical stratification of the water column. Below we discuss potential sources of and possible physiological roles for IPLs in the different zones.

4.1.1 Oxic zone

The glycosyldiacylglycerides that dominate the IPL composition in oxic surface waters, 1G-DAG, 2G-DAG and SQ-DAG, are major constituents of photosynthetic thylakoid and chloroplast membranes

(Wada and Murata, 1998; Siegenthaler, 1998) and are therefore generally assigned to photosynthetic algae or cyanobacteria (Van Mooy et al., 2006; Popendorf et al., 2011b). These are also the likely predominant sources in our study, however, notably 1G-DAG may also be synthesized by heterotrophic bacteria (Popendorf et al., 2011a; Carini et al., 2015; Sebastian et al., 2016). In the oxic zone, 1G- and 2G-DAG are predominantly comprised of C_{16} and C_{18} fatty acids with zero to 5 double bond equivalents polyunsaturated acid (PUFA) combinations such as $C_{16:4}/C_{18:3}$, $C_{16:4}/C_{18:4}$, $C_{18:3}/C_{16:2}$, $C_{18:4}/C_{14:0}$ and $C_{18:5}/C_{14:0}$ (Suppl. Table 5, Fig. 5). These are characteristic of eukaryotic algae (Brett and Müller-Navarra, 1997; Okuyama et al., 1993), such as diatoms and prymnesiophytes that are the major eukaryotic phytoplankton in the ETNP. SQ-DAG biosynthesized by cyanobacteria do not contain PUFA, but instead predominantly contain combinations of $C_{14:0}$, $C_{16:0}$, and $C_{16:1}$ fatty acids (e.g., Siegenthaler, 1998), yielding shorter chain lengths and a lower average number of double bonds (0.5 to 1) than the other glycolipids as observed at the ETNP (Fig. 5). Betaine lipids (DGTS) in surface waters of the ETNP are comprised of C_{14}, C_{16}, C_{18} and C_{20} with multiple unsaturations or rings (on average 1.5 to 3 double bond equivalents) and are also likely phytoplankton derived (Dembitsky, 1996; Popendorf et al., 2011a).

PC-DAG with fatty acyl combinations of $C_{22:6}$ and $C_{20:5}$ long-chain PUFA and $C_{16:0}$ fatty acids (Suppl. Table 5) in surface waters also point to primarily eukaryotic algal sources. PG-DAG is the only phospholipid in cyanobacteria and thylakoid membranes of eukaryotic phototrophs (Wada and Murata, 1998). Heterotrophic bacteria are an additional source for PG-DAG since it can be a major phospholipid in bacterial membranes (Goldfine, 1984). PE-DAG is a minor phospholipid in eukaryotic algae (e.g., Dembitsky et al., 1996) but is common in membranes of bacteria (Oliver and Colwell, 1973; Goldfine, 1984) and is biosynthesized by heterotrophic marine bacteria (Popendorf et al., 2011a). Lower average

504 number of double bond equivalents in PG- and PE-DAG (<2) in the upper water column of the ETNP are
505 consistent with a bacterial origin (Fig. 5).

506 Oxic ETNP waters contain PE- and PC-based phospholipids with mixed acyl and ether core lipids
507 (AEG), which are often referred to as 1-*O*-monoalkyl glycerol ethers (MAGE) if detected as core lipids.
508 PE-AEG have been described in some sulfate-reducing bacteria (Rütters et al., 2001), which in the oxic
509 zone or OMZ of the ETNP would require anoxic microzones in fecal pellets or aggregates (e.g., Bianchi
510 et al., 1992; Shanks and Reeder, 1993). In the ETNP, MAGE-based phospholipids were 1 to 30% of
511 total IPLs. MAGE, detected as core lipids in surface waters of the Southern Ocean and eastern South
512 Atlantic are thought to be breakdown products of IP-AEGs of aerobic bacterial origin (Hernandez-Sanchez
513 et al., 2014), but culturing experiments have yet to confirm this conclusion. Similarly, aerobic bacteria
514 (possibly cyanobacteria) are likely sources for SQ-AEG, since sulfoquinovosyl is a diagnostic headgroup
515 found in cyanobacteria, although, again, these lipids have not been reported in cultured cyanobacteria.
516 Other minor phospholipids in the euphotic zone include PI-DAG and DPG. They are minor components
517 in several marine algae (Dembitsky, 1996) and bacteria (Morita et al., 2010; Diervo et al., 1975;
518 Mileykovskaya and Dowhan, 2009). Bacteria may also be the source of the low detected levels of *N*-
519 methylated phospholipids PME-DAG and PDME-DAG (Goldfine and Ellis, 1964). 3G-DAG comprised
520 of C_{14}, C_{16} and C_{18} fatty acids with up to six double bond equivalents is another minor IPL detected in the
521 euphotic zone at all stations except for station 5. It has been found in some plants (Hölzl and Dörmann,
522 2007) and some anaerobic gram-positive bacteria (Exterkate and Veerkamp, 1969), which could both be
523 probable sources in the oxic euphotic zone of the ETNP.

524 The sphingolipid, 1G-CER, consists of a sphingosine backbone linked to a fatty acid via an amide

525 bond and was a minor component in the oxic zone (<5% of IPL) at all stations (Fig. 4). Glycosidic
526 ceramides occur in eukaryotic algae such as the coccolithophore *Emiliania huxleyi* (Vardi et al., 2009).
527 We also detected 1G-OH-CER with up to 2 hydroxylations in the core lipid structure (Suppl. Fig. 5).
528 Multiple-hydroxylated sphingoid bases are potential markers of viral infection and cell death in at least
529 some marine phytoplankton, notably *E. huxleyi* (Vardi et al., 2009). We did not, however, find mass
530 spectral evidence for the presence of viral polyhydroxylated 1G-CER, as described by Vardi et al. (2009)
531 and therefore rather suggest that eukaryotic algal cells are potential sources for the 1G-CER (Lynch and
532 Dunn et al., 2004) in surface waters of the ETNP. We also detected hydroxylated glycolipids (1G-OH-
533 DAG) and aminolipids (OH-DGTS) with up to two hydroxyl-groups or one hydroxyl group combined
534 with an epoxy or keto function attached to the acyl groups (Suppl. Fig. 5). The addition of hydroxyl
535 groups or general oxidation of fatty acids in plants, algae and yeast is a defense mechanism and response
536 to oxidative stress (Kato et al., 1984; Andreou et al., 2009). Hydroxy fatty acids, for example, are
537 intermediates in oxidative degradation of fatty acids (Lehninger, 1970), and since they are constituents of
538 structural biopolymers of many microorganisms (Ratledge and Wilkinson, 1988), they are present in
539 marine particulate matter (e.g., Wakeham, 1999), likely derived from membrane constituents of Gram-
540 negative bacteria, the most abundant bacteria in seawater (Rappé and Giovannoni, 2000).
541
542 *4.1.2 Upper OMZ*
543 Glycolipid abundance varied between 15 to 80% of total IPL within the upper OMZ below the
544 thermocline/oxycline. SQ-DAG and 2G-DAG exhibited strong decreases in relative and absolute
545 abundance below 125 m at all stations consistent with the decrease in their phototrophic biomass.

546 Number of carbon atoms in the core lipid chains and number of double bond equivalents of glycolipids
547 showed considerable variations within the upper OMZ (Fig. 5), indicating a different assemblage of source
548 organisms compared to the oxic zone. Likewise, decreasing carbon numbers and double bond
549 equivalents for PC-DAG and DGTS combined with a dominance by C_{14}, C_{16} and C_{18} saturated and
550 monounsaturated fatty acids (Suppl. Table 5) supports a shift from eukaryotic to bacterial sources. This
551 suggests the diverse proteobacteria in the upper OMZ may biosynthesize non-phosphorus substitute IPLs.
552 1G-DAG or DGTS are known to replace phospholipids, primarily PE-DAG and PC-DAG under
553 phosphorus limited growth (Geske et al., 2012; Carini et al., 2015; Sebastian et al., 2016; Yao et al., 2015),
554 including at the phosphate concentrations of 2 to 2.5 μM in the upper OMZ. Sulfate-reducing
555 proteobacteria, which comprise up to 10% of the total bacteria in the ETNP (Podlaska et al., 2012) may
556 be candidate organisms for this phospholipid to glycolipid replacement (Bosak et al., 2016). Structures
557 of minor IPLs, AL-I and AL-II were not fully elucidated (see Suppl. Fig. 6) and their origins remain
558 uncertain. PME- and PDME-DAG, DPG, 1G-CER and 1G-OH-CER within the upper OMZ are
559 consistent with previous reports of their production by (unidentified) bacteria near redox boundaries in
560 other stratified water bodies (Schubotz et al., 2009; Wakeham et al., 2012).

561 Archaeal IPLs with glycosidic headgroups and tetraether core structures (1G- and 2G-GDGT)
562 comprised a greater proportion of the overall IPL pool within the upper OMZ than in surface waters.
563 Analysis of these same samples by Xie et al. (2014) first reported that concentrations of glycosidic GDGTs
564 peak in the ETNP roughly at depths where nitrite maxima are observed. IP-GDGTs with the hexose-
565 phosphate-hexose (HPH) headgroups and the core GDGT crenarchaeol (Suppl. Fig. 4) of thaumarchaeota
566 (Schouten et al., 2008; Elling et al., 2017) were most abundant at depths of nitrate maxima at all ETNP

567 stations, as they are in other oxygen-deficient water columns (e.g., Pitcher et al., 2011; Lengger et al.,
568 2012; Schouten et al., 2012; Sollai et al., 2015), although they were present at greater depths in the ENTP
569 as well. The microbial enumerations by Podlaska et al. (2012) had shown previously that
570 thaumarchaeota (referred to as crenarchaeota) and euryarchaeota constitute almost equal amounts to <10%
571 of total cell number in the upper OMZ of the ETNP. It is also possible that uncultured marine Group II
572 euryarchaeota are additional sources for glycosidic GDGTs as has been suggested previously (Lincoln et
573 al., 2014; Zhu et al., 2016).
574
575 *4.1.3 Core OMZ and deep oxycline*
576 IPL distributions in the core OMZ and at the deep oxycline of the ETNP that were notably different
577 from the oxic zone and the upper OMZ are consistent with *in-situ* microbial origins. We choose to
578 discuss the core OMZ and deep oxycline together because, although oxygen concentrations are beginning
579 to rise in the deep oxycline, IPL compositions in both zones are similar and likely reflect similar
580 biogeochemical sources. Phospholipid abundance at all stations generally increased to over 50% (except
581 for station 8) at the expense of glycolipids. PE and PG-DAG are the most abundant phospholipids in the
582 core OMZ, along with PC-DAG and PE- and PC-AEG, DPG. PME and PDME-DAG are all common
583 lipids in α-, γ- and some β-proteobacteria (Oliver and Colwell, 1973; Goldfine, 1984) that are present in
584 the OMZ (Podlaska et al., 2012). Changes in phospholipids chain length and number of double bond
585 equivalents further support *in-situ* IPL production (Fig. 5). Fatty acid combinations for phospholipids
586 were dominated by saturated $C_{14:0}$, $C_{15:0}$ and $C_{16:0}$ and monounsaturated $C_{16:0}$ C_{17} and $C_{18:0}$ (Suppl. Table
587 5); PUFA were generally of reduced abundance, and odd-numbered fatty acids increased in proportion.

588 In the case of PUFA, even though they may be biosynthesized by piezophilic aerobic deep-sea bacteria
589 (DeLong and Yayanos,1986, Fang et al. 2003; Valentine and Valentine, 2004), either the microaerophilic
590 bacteria in the deep OMZ of the ETNP do not produce PUFA or these labile fatty acids are rapidly degraded
591 *in-situ* (DeBaar et al., 1983; Prahl et al., 1984; Neal et al., 1986).

592 Among glycolipids, 1G-DAG was most abundant at the deep OMZ/oxycline at stations 1 and 8; here
593 1G-DAG abundance actually increases over that of shallower depths. Carbon number and number of
594 double bond equivalents for glycolipids are again distinct from the surface waters, with on average 1 to 2
595 carbon atoms shorter chain lengths and 1 to 3 fewer double bonds (Fig. 5), supporting the notion that at
596 least some of these glycolipids are biosynthesized *in-situ* and not simply exported from the surface waters.
597 In particular, SQ-DAG in the core OMZ/oxycline contained odd-carbon numbered fatty acids (e.g.,
598 $C_{15:0}/C_{16:0}$ and $C_{14:0}/C_{15:0}$) different from the cyanobacterial SQ-DAG in surface waters (Suppl. Table 5).
599 Some Gram-positive bacillus and firmicutes biosynthesize 1G, 2G- and SQ-DAG (Hölzl and Dörmann,
600 2007) and 1G-, 2G- and SQ-DAG in deeply buried Wadden Sea sediments are attributed to anaerobic
601 bacteria (Seidel et al., 2012). However, Gram-positive bacteria are generally not abundant in seawater.

602 The core OMZ/deep oxycline are particularly enriched in archaeal GDGT, notably 1G-GDGT and
603 HPH-GDGT, with predominantly GDGT-0 and crenarchaeol as core lipids (Suppl. Fig. 4). At stations 1
604 and 8 where sampling penetrated below ~800 m depth, 1G-GDGT and HPH-GDGT constitute up to ~60%
605 and ~22%, respectively, of total IPL. Significantly, the elevated abundances of 1G-GDGT and HPH-
606 GDGT at the bottoms of the sampling depth profiles in the deep oxycline of stations 1 and 8 correspond
607 to depths at which ammonium concentrations are higher than shallower in the core OMZ (Fig. 2).
608 Remineralization at the deep-oxycline might provide additional ammonium to drive thaumarchaeotal

609 ammonium oxidation and production of archaeal IPLs.

610

611 *4.2 Factors influencing IPL distribution in the ENTP*

612 *4.2.1 Factors affecting structural diversity of the core lipid composition*

613 IPL in the ETNP display considerable diversity not only in the headgroup but also core lipid types,
614 from diacylglycerol lipids with varying number of carbon atoms (likely chain lengths) and zero to multiple
615 double bond equivalents (likely reflecting the number of unsaturations), with or without hydroxylations
616 to mixed ether/ester glycerolipids, sphingolipids and ornithine lipids. Statistical analysis provides aids
617 in illuminating influences of environmental factors and microbial community structure on the lipid
618 composition in the water column of the ETNP. Changes in core alkyl lipid chain length and degree of
619 unsaturation are often associated with temperature (Neidleman, 1987), even at the range of temperatures
620 of the ETNP water column. However, NMDS analysis did not yield any strong correlations between
621 temperature and number of carbon atoms in the side chains or double bond equivalents of the major IPL
622 classes ($r^2 < 0.02$, Suppl. Table 6), nor with other environmental parameters (r2 < 0.3, Suppl. Table 6).
623 Instead, changing biological sources may play a decisive role in determining number of carbon atoms and
624 double bond equivalents in the ETNP. For instance, long-chain PUFAs in surface waters are mainly
625 synthesized by phytoplankton, while in deeper waters some bacteria may biosynthesize these PUFAs.
626 The degree of hydroxylation in the acyl side chains also did not show any clear link to specific
627 environmental factors, although, both 1G-OH-CER and OH-DGTS had negative loadings on the NMDS-
628 2 axis indicating a higher abundance of these compounds in oxic samples. It is possible that hydroxylated
629 IPLs play a role during oxidative stress and/or are involved in other defense mechanisms (Kato et al.,

630 1984; Andreou et al., 2009).

631 Mixed ether-acyl lipids have been reported in various oceanic settings (Hernandez-Sanchez et al.,
632 2014). In our study, there was no noticeable correlation between PE- and PC-AEG and depth or oxygen
633 concentrations (Fig. 6). Ornithine lipids were strongly negatively loaded on the NMDS-1 axis, but none
634 of the measured environmental parameters could account for this negative loading (Fig. 6). Therefore,
635 it remains unclear what factor(s) ultimately determine their distribution. Likewise, there were no
636 significant correlations between the sphingolipid 1G-CER and any environmental parameter. Since
637 ether-acyl lipids, ornithine lipids and sphingolipids play many functional roles in biological systems, their
638 variable distribution within the water column reflect most likely the diversity of microbes inhabiting the
639 dynamic oxygen regime of the ETNP.

640

641 *4.2.2 Factors influencing head group composition*

642 NMDS analysis of normalized IPL composition and quantitative microbial data (abundance of α, β,
643 γ, ε-proteobacteria, sulfate-reducing bacteria δ-proteobacteria, planctomycetes, crenarchaeota including
644 thaumarchaeota and euryarchaeota) did not yield any high goodness of fit statistic ($r^2 < 0.3$; Suppl. Table
645 6) that would clearly delineate specific prokaryotic sources for the various IPL. This absence of
646 statistical correlation would result if neither the IPL compositions of SPM nor the structure and lipid
647 composition of the prokaryotic community were sufficiently unique to strongly distinguish the
648 biogeochemical zones. Indeed, although there are depth-related differences in IPL composition of SPM
649 and prokaryotic community, there is considerable overlap. Therefore, instead of trying to elucidate
650 specific IPL sources, we here query the affect environmental factors such as temperature, nutrient or

651 oxygen concentrations may have on the IPL compositions in the ENTP, and by analogy to natural marine
652 settings in general. Most the major and minor glycolipids were loaded negatively on the NMDS2 axis,
653 as were oxygen, fluorescence, Chl-*α*, POC and TN (Fig. 6). A notable exception was 1G-DAG which
654 had only a slightly negative loading on the NMDS-2 axis. These relationships (loadings) roughly reflect
655 the vertical distribution of IPLs in the water column of the ETNP. Glycolipids, particularly 2G-DAG
656 and SQ-DAG, were most abundant in the euphotic oxic zone characterized by high oxygen concentration
657 and moderate primary productivity, dominated by phytoplankton, primarily cyanobacteria (high POC, TN
658 and elevated Chl-*α* and fluorescence). Spearman Rank Order Correlations confirm these observations,
659 including the lack of significant correlations between 1G-DAG and depth or any other environmental
660 parameter. One explanation is that 1G-DAG originates from assorted sources throughout the water
661 column independent of any single environmental variable. Similarly, PC-DAG, PG-DAG, and DGTS
662 did not correlate with any of the tested environmental variables, because their compositions are relatively
663 homogeneous across all biogeochemical zones. PE-, PME- and PDME-DAG, and DPG, on the other
664 hand, that became more prevalent within the core OMZ, and at deeper depths where oxygen concentrations
665 decrease and nutrient (NO_3^- and PO_4^{3-}) concentrations were elevated due to organic matter
666 remineralization, gave positive loadings with these environmental parameters on the NDMS2 axis.
667 Archaeal IPLs showed positive loadings on the NMDS2 axis, consistent with the increasing importance
668 of archaeal abundance with depth and at reduced oxygen concentrations.
669
670 *4.2.3 Links between substitute lipid ratios and nutrient concentrations*
671 SQ-DAG and PC-DAG are often the most abundant respective glycolipids and phospholipids in the

672 surface ocean (Popendorf et al., 2011a,b), including the Eastern Tropical South Pacific (Van Mooy and
673 Fredricks, 2010). The abundance of SQ-DAG in the surface waters of the ETNP (18-50% of total IPL)
674 is thus not unusual. In the ETNP, however, PC-DAG was comparably minor (3-13% of total IPL).
675 Instead, DGTS was abundant at some stations, up to ~20% of major IPL at station 5. SQ-DAG and
676 DGTS serve similar biochemical functions as the phospholipids PG-DAG and PC-DAG, respectively, due
677 to similar ionic charges at physiological pH. The former may be preferentially biosynthesized by
678 phytoplankton and some bacteria as substitute lipids for PG-DAG and PC-DAG when phosphate starved
679 (Benning, 1993; Van Mooy et al., 2006, 2009). Likewise, 1G-DAG, glycuronic acid diacylglycerol
680 (GADG) and ornithine lipids may substitute for PE-DAG in marine bacteria (e.g., chemoheterotrophic α-
681 proteobacteria of the SAR11 clade of *Pelagibacter* sp.: Carini et al., 2015; the sulfate reducing bacterium,
682 *Desulfovibrio alaskensis*: Bosak et al., 2016). In oligotrophic surface waters of the Sargasso Sea (PO_4^{3-}
683 <10 nM) ratios of SQ-DAG:PG-DAG and DGTS:PC-DAG are high (4 to 13) compared to the same ratios
684 (3) in the phosphate replete South Pacific (PO_4^{3-} >100 nM), consistent with cyanobacteria synthesizing
685 phosphorus-free substitute lipids to maintain growth in response to phosphorus deprivation (Van Mooy et
686 al., 2009). At the ETNP, SQ-DAG:PG-DAG ratios ranged between 1 and 10 within the upper 100-200
687 m along the transect and were <1 deeper into the OMZ (Fig. 3). DGTS:PC-DAG ratios in the ETNP
688 were quite variable, ranging between 0.4 and 2.4 at most depths, but with notable spikes (>30) within the
689 oxic zone at station 5, within the upper core OMZ at station 2 and 8 and in the lower portion of the core
690 OMZ at station 8. 1G-DAG:PE-DAG ratios where highly variable (0.2 to 945) and were highest within
691 the upper OMZ at station 2, 5 and 8 and within the deep oxycline at station 8, where 1G-DAG:PE ratios
692 range between 290 and 945 (Fig. 3). To test the substitute lipid hypothesis for the ETNP, we performed

693 a Spearman Rank Order Correlation analysis of known substitute lipid ratios as well as total aminolipid
694 (AL) to phospholipid (PL) and total glycolipid (GL) to PL ratios with nutrient concentrations and other
695 environmental parameters. Only SQ-DAG:PG-DAG was significantly correlated with phosphate (-0.56,
696 $p<0.001$) but also correlated with other parameters, such as depth (-0.76, $p<0.001$) and oxygen
697 concentration (0.58, $p<0.001$). These correlations reflect the elevated SQ-DAG:PG-DAG ratios (2-8) in
698 the surface waters and upper OMZ (Fig. 3) and support the notion that SQ-DAG might serve as a substitute
699 lipid in both surface waters and the OMZ when phosphate concentrations are in the low micromolar range
700 (~0.1-0.4 μM in surface waters; ~2-3.5 μM in the OMZ). Other proposed substitute lipid ratios,
701 DGTS:PC-DAG (Van Mooy et al., 2009) and 1G-DAG:PE-DAG (Carini et al., 2015), did not correlate
702 with nutrient concentrations in the water column of the ETNP but rather showed highly variable
703 distributions. Similarly, AL:PL ratios did not exhibit strong relationships with any environmental
704 parameter, and GL:PL ratios showed similar but less pronounced trends as SQ-DAG:PG-DAG ratios.
705 Overall, we observed no correlation between these substitute lipid ratios and phosphate concentration in
706 the ETNP. We propose that non-phosphorus IPL within the OMZ of the ETNP originate from bacteria
707 growing under low micromolar concentrations of phosphate. Indeed, the culture experiments of Bosak
708 et al. (2016) demonstrated that the sulfate reducer, *Desulfovibrio alaskensis*, begins to replace most of its
709 membrane phospholipids with 1G-DAG, glycuronic acid diacylglycerol and ornithine lipids even at
710 phosphate concentrations as high as 20 μM.
711
712 **5. Conclusions**
713 The water column of the ETNP is characterized by a diverse suite of intact polar lipids. IPL

714 distributions reflect the dynamic nature of the biological community in the ETNP, with light and oxygen
715 as primary determinants, from fully oxygenated euphotic surface waters to an aphotic strong oxygen
716 minimum zone at mid-depth. Highest concentrations of IPLs (250 – 1500 ng/L) in oxygenated surface
717 waters zone results from abundant phototrophic eukaryotic and cyanobacterial sources above the OMZ.
718 Secondary peaks in IPL concentration (12 – 56 ng/L) within the core of the OMZ mirror elevated
719 abundances of heterotrophic and chemoautotrophic bacteria and archaea under low oxygen conditions.
720 Glycolipids derived from photoautotrophs generally accounted for more than 50% of total IPLs in the
721 euphotic zone (< 200 m, oxic and upper OMZ zones), but bacterial phospholipids were more abundant
722 (avg. 40%) in the OMZ and deep oxycline layers. Archaeal GDGTs were abundant within the OMZ and
723 deep oxycline, consistent with elevated archaeal cell abundances there. Variations in major fatty acid
724 constituents within IPL classes with acyl core moieties show that biological source(s) for the different IPL
725 were distinct in each depth/oxygen-content horizon. Nevertheless, microbial sources for many of the
726 detected lipids remain unclear and therefore potentially unique ecophysiological adaptations these lipids
727 may represent remain to be explored.

728 The presence of the glycolipid, monoglycosyl diacylglycerol (1G-DAG), and the betaine lipid,
729 diacylglyceryl homoserine (DGTS), both with varying fatty acid compositions, within all biogeochemical
730 zones, and especially in the OMZ, indicates that these canonical phototrophic markers are not only
731 biosynthesized in surface waters, but may indeed be produced in the aphotic water column and by a much
732 larger host of organisms than previously thought. Since 1G-DAG and DGTS can be biosynthesized by
733 various bacteria to replace phospholipids under phosphorus limited growth, we suggest that they serve as
734 non-phosphorus substitute lipids for some microorganisms in the OMZ. The presence of these substitute

735 lipids at micromolar concentrations of phosphate of the ETNP suggests that the paradigm of substitute
736 lipid biosynthesis being restricted to the PO_4^{3-}-depleted oligotrophic surface ocean may need to be re-
737 evaluated.

738

739 **Author contribution**

740 SGW collected the samples. SGW, FS and KUH designed the study. SX and FS measured and processed
741 the data. JSL and FS performed statistical analyses. FS and SGW wrote the paper with input from SX,
742 KUH and JSL.

743

744 **Competing interests**

745 The authors declare that they have no conflict of interest.

746

747 **Acknowledgments**

748 We are grateful to the captain and the crew of R/V *Seward Johnson*, to K. Daly and K. Wishner as co-
749 chief scientists, and to the U.S. National Science Foundation for supporting the cruise. H. Albrecht, B.
750 Olsen and S. Habtes helped with PM sampling. We thank K. Fanning and R. Masserini (University of
751 South Florida) for providing their nutrient results; C. Flagg (Stony Brook) processed CTD hydrographic
752 data; Jay Brandes and Mary Richards (Skidaway Institute) conducted the POC and TN analyses; B. Olson
753 and K. Daly (University of South Florida) provided ship-board Chl-*a* analyses; and G. DeTullio (College
754 of Charleston) conducted HPLC analyses of pigments. Lab supplies and analytical infrastructure for
755 lipid analyses was funded by the Deutsche Forschungsgemeinschaft (DFG, Germany) through the Cluster

of Excellence/Research Center MARUM. The UHPLC-QTOF instrument was granted by the DFG, Germany through grants Inst 144/300-1. S. Xie was funded by the China Scholarship Council, F. Schubotz by the Zentrale Forschungsförderung of the University of Bremen, and U.S. National Science Foundation grant OCE-0550654 to S. G. Wakeham supported this project. SGW also acknowledges a Fellowship from the Hanse-Wissenschaftskolleg (Hanse Institute for Advanced Studies) in Delmenhorst, Germany.

References

Andreou, A., Brodhun, F., Feussner, I.: Biosynthesis of oxylipins in non-mammals, Progr. Lip. Res., 48, 148-170, 2009.

Bale, N. J., Hopmans, E. C., Schoon, P. L., de Kluijver, A., Downing, J. A., Middelburg, J. J., Sinninghe Damsté, J. S. and Schouten, S.: Impact of trophic state on the distribution of intact polar lipids in surface waters of lakes. Limnol. Oceanogr., 61, 1065–1077, 2016.

Basse, A., Zhu, C., Versteegh, G.J.M., Fischer, G., Hinrichs, K.-U., and Mollenhauer, G.: Distribution of intact and core tetraether lipids in water column profiles of suspended particulate matter off Cape Blank, NW Africa, Org. Geochem., 72, 1-13, 2014.

Benning, C., Beatty, J. T., Prince, R. C., and Somerville C. R.: The sulfolipid sulfoquinovosyldiacylglycerol is not required for photosynthetic electron transport in Rhodobacter sphaeroides but enhances growth under phosphate limitation, Proc. Natl. Acad. Sci. USA, 90, 1561–1565, 1993.

Bianchi, M., Marty, D., Teyssié, J.-L., and Fowler, S. W.: Strictly aerobic and anaerobic bacteria

777 associated with sinking particulate matter and zooplankton fecal pellets, Mar. Ecol. Press Ser., 88, 55-
778 60, 1992.
779 Bosak, T., Schubotz, F., de Santiago-Torio, A., Kuehl, J. V., Carlson, H. K., Watson, N., Daye, M.,
780 Summons, R. E., Arkin, A. P., and Deutschbauer A. M.: System-wide adaptations of *Desulfovibrio*
781 *alaskensis* G20 to phosphate-limited conditions, PLoS ONE 11, e0168719, 2016.
782 Brandsma, J., Hopmans, E. C., Philippart, C. J. M., Veldhuis, M. J. W., Schouten, S., and Sinninghe
783 Damste, J. S.: Low temporal variation in the intact polar lipid composition of North Sea coastal marine
784 water reveals limited chemotaxonomic value, Biogeosciences, 9, 1073–1084, 2012.
785 Brett, M. T., and Müller-Navarra, D. C.: The role of highly unsaturated fatty acids in aquatic foodweb
786 pro- cesses, Freshw. Biol., 38, 483–499, 1997.
787 Carini P., Van Mooy B. A. S., Thrash J. C., White A., Zhao Y., Campbell E. O., Fredricks H. F., and
788 Giovannoni S. J.: SAR11 lipid renovation in response to phosphate starvation. Proc. Natl. Acad. Sci.
789 USA, 112, 7767–7772, 2015.
790 Carolan, M.T., Smith, J.M., and Beman, J.M.: Transcriptomic evidence for microbial sulfur cycling in the
791 eastern tropical North Pacific oxygen minimum zone. Front. Microbiol. 6, 334, 2015.
792 Cass, C. J., and Daly, K. L.: Ecological characteristics of eucalanoid copepods of the eastern tropical
793 North Pacific Ocean: Adaptations for life within a low oxygen system, J. Exp. Mar. Biol. Ecol., 468,
794 118-129, 2015.
795 Cavan, E. L., Trimmer, M., Shelley, F., Sanders, R.: Remineralization of particulate organic carbon in an
796 ocean oxygen minimum zone, Nat. Comm., 8, 14847, 2016.
797 Codispoti, L. A., and Richards, F. A.: An analysis of the horizontal regime of denitrification in the eastern

798 tropical North Pacific. Limnology and Oceanography 21, 379-388, 1976.
799 DeBaar, H. J. W., Farrington, J. W. and Wakeham, S. G.: Vertical flux of fatty acids in the North Atlantic
800 Ocean, J. Mar. Res., 41, 19-41, 1983.
801 DeLong, E. F. and Yayanos, A.: Biochemical function and ecological significance of novel bacterial lipids
802 in deep-sea procaryotes, Appl. Environ. Mirobiol., 51, 730-737, 1986.
803 Dembitsky, V.: Betaine ether-linked glycerolipids: Chemistry and biology, Progr. Lip. Res., 35, 1-51,
804 1996.
805 Diervo, A. J. and Reynolds, J. W.: Phospholipid composition and cardiolipin synthesis in fermentative
806 and nonfermentative marine bacteria, J. Bacteriol. 123, 294-301, 1975.
807 DiTullio, G., and Geesey, M. E.: Photosynthetic Pigments in Marine Algae and Bacteria. In: G Bitton (ed),
808 Encyclopedia of Environmental Microbiology, vol. 5, Wiley, pp 2453-2470, 2002.
809 Elling, F. J., Könneke, M., Mußmann, M., Greve, A., and Hinrichs, K.-U.: Influence of temperature, pH,
810 and salinity on membrane lipid composition and TEX86 of marine planktonic thaumarchaeal isolates,
811 Geochim. Cosmochim. Acta, 171, 238-255, 2015.
812 Elling, F. J., Könneke, M., Nicol, G. W., Stieglmeier, M., Bayer, B., Spieck, E., La Torre, De J. R., Becker,
813 K. W., Thomm, M., Prosser, J. I., Herndl, G. J., Schleper, C., and Hinrichs, K.-U. Chemotaxonomic
814 characterisation of the thaumarchaeal lipidome, Environ. Microbiol. 10, 1080, 2017.
815 Ertefai, T., Fisher, M., Fredricks, H. and Lipp, J.: Vertical distribution of microbial lipids and functional
816 genes in chemically distinct layers of a highly polluted meromictic lake, Org. Geochem., 39, 1572-
817 1588, 2008.
818 Exterkate, F. A., and Veerkamp, J. H.: Biochemical changes in Bifidobacterium bifidum var.

819 Pennsylvanicus after cell wall inhibition. I. Composition of lipids, Biochim. Biophys. Acta, 176, 65–
820 77, 1969.
821 Fang, J., Kato, C., Sato, T., Chan, O., and McKay, D.: Biosynthesis and dietary uptake of polyunsaturated
822 fatty acids by piezophilic bacteria. Comp. Biochem. Physiology Part B, 137 455–46, 2004.
823 Fiedler, P. C., and Talley, L. D.: Hydrography of the eastern tropical Pacific: A review. Progr. Oceanogr.,
824 69, 143-180, 2006.
825 Franck, V. M., Smith, G. J., Bruland, K. W., and Brzezinski, M. A.: Comparison of size-dependent carbon,
826 nitrate and silicic acid uptake rates in high- and low-iron waters. Limnol. Oceanogr., 50, 825-838,
827 2005.
828 Geiger, O., González-Silva, N., López-Lara, I. M., and Sohlenkamp, C.: Amino acid-containing
829 membrane lipids in bacteria, Progr. Lip. Res., 49, 46–60, 2010.
830 Geiger, O., Röhrs, V., Weissenmayer, B., Finan, T. M., and Thomas-Oates, J. E.: The regulator gene phoB
831 mediates phosphate stress-controlled synthesis of the membrane lipid diacylglyceryl-N,N,N-
832 trimethylhomoserine in Rhizobium (Sinorhizobium) meliloti, Mol. Microbiol., 32, 63–73, 1999.
833 Geske, T., Dorp vom, K., Dörmann, P., and Hölzl G.: Accumulation of glycolipids and other non-
834 phosphorous lipids in Agrobacterium tumefaciens grown under phosphate deprivation, Glycobiol., 23,
835 69–80, 2012.
836 Goericke, R., Olson, R. J., and Shalapyonok, A.: A novel niche for Prochlorococcus sp. in low-light
837 suboxic environments in the Arabian Sea and the Eastern Tropical North Pacific, Deep Sea Res. I, 47,
838 1183-1205, 2000.
839 Goldfine, H.: Bacterial membranes and lipid packing theory, J. Lip. Res., 25, 1501–1507, 1984.

840 Goldfine, H., and Ellis, M. E.: N-methyl groups in bacterial lipids, J. Bacteriol., 87, 8–15, 1964.
841 Gruber, N.: The marine nitrogen cycle: overview and challenges, in: Nitrogen in the marine environment,
842 Eds. DG Capone, DA Bronk, MR Mulholland, EJ Carpenter, Burlington, MA, USA: Academic, 1-50,
843 2008.
844 Harvey, R. H., Fallon R. D., and Patton, J. S.: The effect of organic matter and oxygen on the degradation
845 of bacterial membrane lipids in marine sediments, Geochim. Cosmochim. Acta, 50, 795-804, 1986.
846 Hernandez-Sanchez, M. T., Homoky, W. B., and Pancost, R. D.: Occurrence of 1-O-monoalkyl glycerol
847 ether lipids in ocean waters and sediment, Org. Geochem. 66, 1–13, 2014.
848 Hölzl, G., and Dörmann, P.: Structure and function of glycoglycerolipids in plants and bacteria, Progr.
849 Lip. Res. 46, 225–243, 2007.
850 Hurley, S. J., Elling, F. J., Könneke, M., Buchwald, C., Wankel, S. D., Santoro, A. E., Lipp, J. S., Hinrichs,
851 K.-U., and Pearson, A.: Influence of ammonia oxidation rate on thaumarchaeal lipid composition and
852 the TEX86 temperature proxy, Proc. Natl. Acad. Sci. USA, 113, 7762-7767, 2016.
853 Kalvelage, T., Lavik, G., Jensen, M. M., Revsbech, N. P., Löscher, C., Schunck, H., Desai, D. K., Hauss,
854 H., Kiko, R., Holtappels, M., LaRoche, J., Schmitz, R. A., Graco, M. I., and Kuypers, M. M. M:
855 Aerobic microbial respiration in oceanic oxygen minimum zones, PLoS ONE, 10(7):e0133526, 2015.
856 Karstensen, J., Stramma L., and Visbeck M.: Oxygen minimum zones in the eastern tropical Atlantic and
857 Pacific oceans, Progr. Oceanogr., 77, 331-350, 2008.
858 Kato, T., Yamaguchi, Y., Hirano, T., and Yokoyama, T.: Unsaturated hydroxy fatty acids, the self
859 defensive substances in rice plant against rice blast disease, Chem. Let., 409-412, 1984.
860 Keeling, R. F., Körtzinger, A., and Gruber N.: Ocean deoxygenation in a warming world, Annu. Rev.

Marine. Sci., 2, 199–229, 2010.

Kharbush, J. J., Allen, A. E., Moustafa, A., Dorrestein, P.C., Aluwihare, L. I.: Intact polar diacylglycerol biomarker lipids isolated from suspended particulate organic matter accumulating in an ultraoligotrophic water column, Org. Geochem., 100, 29-41, 2016.

Lam, P. and Kuypers, M. M. M.: Microbial nitrogen cycling processes in oxygen minimum zones, Annu. Rev. Marine. Sci., 3, 317–345, 2011.

Landry, M. R., Selph, K. E., Taylor, A.G., Décima, M., Balch, W. M., and Bidigare R. R.: Phytoplankton growth, grazing and production balances in the HNLC equatorial Pacific, Deep Sea Res. I, 58, 524-535, 2011.

Lavín, M. F., Fiedler, P. C., Amador, J. A., Balance, L. T., Färber-Lorda, J., Mestas-Nuñez, A. M.: A review of eastern tropical Pacific oceanography: Summary, Progr. Oceanogr., 69, 391-398, 2006.

Lee C., and Cronin C.: Particulate amino acids in the sea: Effects of primary productivity and biological decomposition, J. Mar. Res., 42, 1075-1097, 1984.

Lehninger A. L.: Oxidation of fatty acids, in: Biochemistry, New York: Worth, 417-432, 1970.

Lengger, S. K., Hopmans, E. C., Sinninghe Damsté, J. S., and Schouten, S.: Comparison of extraction and work up techniques for analysis of core and intact polar tetraether lipids from sedimentary environments, Org. Geochem., 47, 34–40, 2012.

Lin, X., Wakeham, S. G., Putnam, I. F., Astor, Y. M., Scranton, M. I., Chistoserdov, A. Y., and Taylor, G. T.: Comparison of vertical distributions of prokaryotic assemblages in the anoxic Cariaco Basin and Black Sea by use of fluorescence in situ hybridization, Appl. Environ. Microbiol., 72, 2679-2690, 2006.

882 Lincoln, S. A., Wai, B., Eppley, J. M., Church, M. J., Summons, R. E. and DeLong, E. F.: Planktonic
883 Euryarchaeota are a significant source of archaeal tetraether lipids in the ocean, Proc. Natl. Acad. Sci.
884 USA, 111, 9858–9863, 2014.
885 Lynch, D. V., and Dunn, T. M.: An introduction to plant sphingolipids and a review of recent advances in
886 understanding their metabolism and function, New Phytol., 161, 677-702, 2004.
887 Ma, Y., Zeng, Y., Jiao, N., Shi, Y., and Hong, N.: Vertical distribution and phylogenetic composition of
888 bacteria in the Eastern Tropical North Pacific Ocean, Microbiol. Res., 164, 624-663, 2009.
889 Maas, A. E., Frazar, S. L., Outram, D.M., Seibel, B. A., and Wishner, K. F.: Fine-scale vertical
890 distributions of macroplankton and micronekton in the Eastern Tropical North Pacific in association
891 with an oxygen minimum zone, J Plankt. Res., 36, 1557-1575, 2014.
892 Martin, J. H., Knauer, G. A., Karl, D. M., and Broenkow, W. W.: VERTEX: carbon cycling in the northeast
893 Pacific, Deep-Sea Research 34, 267-285, 1987.
894 Matos, A. R., and Pham-Thi, A.-T.: Lipid deacylating enzymes in plants: Old activities, new genes. Plant
895 Physiol. and Biochem. 47, 491-503, 2009.
896 Meador, T. B., Gagen, E. J., Loscar, M. E., Goldhammer, T., Yoshinaga, M. Y., Wendt, J., Thomm, M.,
897 and Hinrichs, K.-U.: Thermococcus kodakarensis modulates its polar membrane lipids and elemental
898 composition according to growth state and phosphate availability, Front. Microbiol., 5:10,
899 doi:10.3389/fmicb.2014.00010, 2014.
900 Mileykovskaya, E., and Dowhan, W.: Cardiolipin membrane domains in prokaryotes and eukaryotes,
901 Biochim. Biophys. Acta 1788, 2084–2091, 2009.
902 Morita, Y. S., Yamaryo-Botte, Y., and Miyanagi, K.: Stress-induced synthesis of phosphatidylinositol 3-

903 phosphate in mycobacteria, J. Biol. Chem. 285, 16643-16650, 2010.
904 Neal, A. C., Prahl, F. G., Eglinton, G., O'Hara, S. C. M., and Corner, E. D. S.: Lipid changes during a
905 planktonic feeding sequence involving unicellular algae, Elminius Nauplii and Adult Calanus, J. Mar.
906 Biol. Assoc. UK, 66, 1-13, 1986.
907 Neidleman, S. L.: Effects of temperature on lipid unsaturation: Biotechnology and Genetic Engineering
908 Reviews, 5:1, 245-268, 1987.
909 Oliver, J. D., and Colwell, R. R.: Extractable lipids of gram-negative marine bacteria: Phospholipid
910 composition, J. Bacteriol. 114, 897-908, 1973.
911 Olson, M. B., and Daly, K. L.: Micro-grazer biomass, composition and distribution across prey resource
912 and dissolved oxygen gradients in the far eastern tropical north Pacific Ocean, Deep Sea Res. I, 75,
913 28-38, 2014.
914 Okuyama, H., Kogame, K., and Takeda, S.: Phylogenetic significance of the limited distribution of
915 octadecapentaenoic acid in prymnesiophytes and photosynthetic dinoflagellates, Proc. NIPR Symp.
916 Polar Biol., 6, 21–26, 1993.
917 Parsons, T. R., Takahashi, M., and Hargrave B. (Eds.): Biological Oceanographic Processes, 3rd ed.,
918 Pergamon Press, NY, 1984.
919 Paulmier, A., and Ruiz-Pino, D.: Oxygen minimum zones (OMZs) in the modern ocean, Progr. Oceanogr.
920 80, 113-128, 2009.
921 Pennington, J. T., Mahoney, K. L., Kuwahara, V. S., Kolber, D. D., Clienes, R., Chavez, F. P.: Primary
922 production in the eastern tropical Pacific: A review, Progr. Oceanogr., 69, 285-317, 2006.
923 Pitcher, A., Villanueva, L., Hopmans, E. C., Schouten, S., Reichart, G.-J. and Sinninghe Damsté, J. S.:

924 Niche segregation of ammonia-oxidizing archaea and anammox bacteria in the Arabian Sea oxygen
925 minimum zone, ISME J., 5, 1896–1904, 2011.
926 Podlaska, A., Wakeham, S. G., Fanning, K. A., and Taylor, G. T.: Microbial community structure and
927 productivity in the oxygen minimum zone of the eastern tropical North Pacific, Deep-Sea Res. Part I,
928 66, 77–89, 2012.
929 Popendorf, K., Lomas, M., and Van Mooy, B.: Microbial sources of intact polar diacylglycerolipids in the
930 Western North Atlantic Ocean, Org. Geochem. 42, 803-811, 2011a.
931 Popendorf, K. J., Tanaka, T., Pujo-Pay, M., Lagaria, A., Courties, C., Conan, P., Oriol, L., Sofen, L. E.,
932 Moutin, T., and Van Mooy, B. A. S.: Gradients in intact polar diacylglycerolipids across the
933 Mediterranean Sea are related to phosphate availability, Biogeosci. 8, 3733–3745, 2011b.
934 Prahl, F. G., Eglinton, G., Corner, E. D. S., O'Hara, D. C. M., and Forsberg, T. E. V.: Changes in plant
935 lipids during passage through the gut of Calanus, J. Mar. Biol. Assoc. UK, 1984.
936 Rabinowitz, G. B.: An introduction to nonmetric multidimensional scaling, Amer. J. Polit. Sci., 343-90,
937 1975.
938 Rappé, M. S., and Giovannoni, S. J.: The uncultured microbial majority, Annu. Rev. Microbiol., 57, 369-
939 394, 2003.
940 Rojas-Jiménez, K., Sohlenkamp, C., Geiger, O., Martínez-Romero, E., Werner, D., and Vinuesa, P.: A
941 ClC chloride channel homolog and ornithine-containing membrane lipids of rhizobium tropici
942 CIAT899 are involved in symbiotic efficiency and acid tolerance, Mol. Plant-Microbe Interact., 18,
943 1175–1185, 2005.
944 Rush, D., Wakeham, S. G., Hopmans, E. C., Schouten, S., and Damsté, J. S. S.: Biomarker evidence for

945 anammox in the oxygen minimum zone of the Eastern Tropical North Pacific, Org. Geochem., 53,
946 80–87, 2012.
947 Rütters, H., Sass, H., Cypionka, H., and Rullkötter, J.: Monoalkylether phospholipids in the sulfate-
948 reducing bacteria Desulfosarcina variabilis and Desulforhabdus amnigenus, Arch. Microbiol., 176,
949 435–442, 2011.
950 Schouten, S., Pitcher, A., Hopmans, E. C., Villanueva, L., Van Bleijswijk, J., and Sinninghe Damsté, J.
951 S.: Intact polar and core glycerol dibiphytanyl glycerol tetraether lipids in the Arabian Sea oxygen
952 minimum zone: I. Selective preservation and degradation in the water column and consequences for
953 the TEX86, Geochim. Cosmochim. Acta, 98, 228–243, 2012.
954 Schubotz, F., Wakeham, S. G., Lipp, J., Fredricks, H. F., and Hinrichs, K.-U.: Detection of microbial
955 biomass by intact polar membrane lipid analysis in the water column and surface sediments of the
956 Black Sea, Environ. Microbiol., 11, 2720-2734, 2009.
957 Sebastian, M., Smith, A. F., González, J. M., Fredricks, H. F., Van Mooy, B., Koblížek, M., Brandsma,
958 J., Koster, G., Mestre, M., Mostajir, B., Pitta, P., Postle, A. D., Sánchez, P., Gasol, J. M., Scanlan, D.
959 J., and Chen, Y.: Lipid remodelling is a widespread strategy in marine heterotrophic bacteria upon
960 phosphorus deficiency, ISME J, 10, 968–978, 2016.
961 Seibel, B.A.: Critical oxygen levels and metabolic suppression in oceanic oxygen minimum zones, J. Exp.
962 Biol., 214, 326-336, 2011.
963 Seidel, M., Graue, J., Engelen, B., Köster, J., Sass, H., and Rullkötter, J.: Advection and diffusion
964 determine vertical distribution of microbial communities in intertidal sediments as revealed by
965 combined biogeochemical and molecular biological analysis, Org. Geochem., 52, 114–129, 2012.

966 Shanks, A. L., and Reeder, M. L.: Reducing microzones and sulfide production in marine snow. Marine
967 Ecology Press Series 96, 43-47, 1993.
968 Siegenthaler P.-A.: Molecular organization of acyl lipids in photosynthetic membranes of higher plants,
969 in: Lipids in Photosynthesis, Siegenthaler, P.-A., and Murata, N. (Eds). Dordrecht, the Netherlands:
970 Kluwer Academic Publishers, 119–144, 1998.
971 Sohlenkamp, C., López-Lara, I. M., and Geiger, O.: Biosynthesis of phosphatidylcholine in bacteria, Progr.
972 Lip. Res., 42, 115–162, 2003.
973 Sollai, M., Hopmans, E. C., Schouten, S., Keil, R. G., and Sinninghe Damsté, J.S.: Intact polar lipids of
974 Thaumarchaeota and anammox bacteria as indicators of N cycling in the eastern tropical North Pacific
975 oxygen-deficient zone, Biogeosci., 12, 4833-4864, 2015.
976 Stevens H., and Ulloa, O.: Bacterial diversity in the oxygen minimum zone of the eastern tropical South
977 Pacific, Environ. Microbiol., 10, 1244–1259, 2008.
978 Stramma, L., Johnson, G. C., Sprintall, J., and Mohrholz, V.: Expanding Oxygen-Minimum Zones in the
979 Tropical Oceans, Science, 320, 655-658, 2008.
980 Stramma, L., Schmidtko, S., Levin, L. A., and Johnson, G. C.: Ocean oxygen minima expansions and their
981 biological impacts, Deep Sea Res. I, 57, 587-595, 2010.
982 Sturt, H. F., Summons, R. E., Smith, K.E., Elvert, M., Hinrichs, K.-U.: Intact polar membrane lipids in
983 prokaryotes and sediments deciphered by high-performance liquid chromatography/electrospray
984 ionization multistage mass spectrometry - new biomarkers for biogeochemistry and microbial ecology,
985 Rapid Comm. Mass Spec., 18, 617-628, 2004.
986 Taylor, G. T., Iabichella, M., Ho, T.-Y., Scranton, M. I., Thunell, R. C., Muller-Karger, F., and Varela R.:

Chemoautotrophy in the redox transition zone of the Cariaco Basin: A significan midwater source of organic carbon production, Limol. Oceanogr., 46, 148-163, 2001.

Tiano, L., Garcia-Robledo, E., Dalsgaard, T., Devol, A. H., Ward, B. B., Ulloa, O., Canfield, D. E., and Revsbech, N. P.: Oxygen distribution and aerobic respiration in the north and south eastern tropical Pacific oxygen minimum zones, Deep Sea Res. I, 94, 173-183, 2014.

Turich, C., and Freeman, K. H.: Archaeal lipids record paleosalinity in hypersaline systems, Org. Geochem. 42, 1147-1157, 2011.

Ulloa, O., Canfield, D., DeLong, E. F., Letelier, R. M., and Stewart, F. J.: Microbial oceanography of anoxic oxygen minimum zones, Proc. Natl. Acad. Sci., USA 109, 15996-16003, 2012.

Valentine, R. C., and Valentine, D. L.: Omega-3 fatty acids in cellular membranes: a unified concept, Progr. Lip. Res. 43, 383–402, 2004.

Van Mooy, B. A. S., and Fredricks, H. F.: Bacterial and eukaryotic intact polar lipids in the eastern subtropical South Pacific: Water-column distribution, planktonic sources, and fatty acid composition, Geochim. Cosmochim. Acta, 74, 6499–6516, 2010.

Van Mooy, B. A. S., Fredricks, H. F., Pedler, B. E., Dyhrman, S. T., Karl, D. M., Koblížek, M., Lomas, M. W., Mincer, T. J., Moore, L. R., Moutin, T., Rappé, M. S., and Webb, E. A.: Phytoplankton in the ocean use non-phosphorus lipids in response to phosphorus scarcity, Nature, 458, 69–72, 2009.

Van Mooy, B. A. S., Rocap, G., Fredricks, H. F., Evans, C. T., and Devol, A. H.: Sulfolipids dramatically decrease phosphorus demand by picocyanobacteria in oligotrophic marine environments, Proc. Natl. Acad. Sci. USA, 103, 8607–8612, 2006.

Vardi, A., Van Mooy, B. A. S., Fredricks, H. F., Popendorf, K. J., Ossolinski, J. E., Haramty, L., and Bidle,

1008 K. D.: Viral glycosphingolipids induce lytic infection and cell death in marine phytoplankton, Science,
1009 326, 861-865, 2009.
1010 Wada, H., and Murata, N.: Membrane Lipids in cyano- bacteria, in: Lipids in Photosynthesis: Structure,
1011 Function and Genetics, Siegenthaler, P., and Murata, N. (Eds), Dordrecht, the Netherlands: Kluwer
1012 Academic Publishers, 65–81, 1998.
1013 Wakeham, S. G., Turich, C., Schubotz, F., Podlaska, A., Li, X. N., Varela, R., Astor, Y., Sáenz, J. P.,
1014 Rush, D., Sinninghe Damsté, J. S., Summons, R. E., Scranton, M. I., Taylor, G. T., and Hinrichs, K.-
1015 U.: Biomarkers, chemistry and microbiology show chemoautotrophy in a multilayer chemocline in
1016 the Cariaco Basin, Deep Sea Res. Part I, 63, 133–156, 2012.
1017 Wakeham, S. G., Amann, R., Freeman, K. H., Hopmans, E. C., Jørgensen, B. B., Putnam, I. F., Schouten,
1018 S., Sinninghe Damsté, J. S., Talbot, H. M., and Woebken, D.: Microbial ecology of the stratified water
1019 column of the Black Sea as revealed by a comprehensive biomarker study, Org. Geochem., 38, 2070–
1020 2097, 2007.
1021 Wakeham. S. G.: Monocarboxylic, dicarboxylic and hydroxy acids released by sequential treatments of
1022 suspended particles and sediments of the Black Sea, Org. Geochem. 30, 1059-1074, 1999.
1023 Wakeham, S. G.: Reduction of stenols to stanols in particulate matter at oxic-anoxic boundaries in sea
1024 water, Nature, 342, 787-790, 1989.
1025 Wakeham, S. G., and Canuel, E. A.: Organic geochemistry of particulate matter in the eastern tropical
1026 North Pacific Ocean: Implications for particle dynamics, J. Mar. Res., 46, 182-213, 1988.
1027 Wakeham, S. G.: Steroid geochemistry in the oxygen minimum zone of the eastern tropical North Pacific
1028 Ocean, Geochim. Cosmochim. Acta, 51, 3051-3069, 1987.

1029 Williams, R. L., Wakeham, S., McKinney, R., Wishner, K. F.: Trophic ecology and vertical patterns of
1030 carbon and nitrogen stable isotopes in zooplankton from oxygen minimum zone regions, Deep Sea
1031 Res. I, 90 36-47, 2014.
1032 Wishner, K. F., Outram, D. M., Seibel, B. A., Daly, K. L., and Williams, R. L.: Zooplankton in the eastern
1033 tropical north Pacific: Boundary effects of oxygen minimum zone expansion, Deep Sea Res. I, 79,
1034 122-140, 2013.
1035 Wishner, K. F., Gelfman, C., Gowing, M. M., Outram, D. M., Rapien, M., and Williams, R. L.: Vertical
1036 zonation and distributions of calanoid copepods through the lower oxycline of the Arabian Sea oxygen
1037 minimum zone, Progr. Oceanogr., 78, 163-191, 2008.
1038 Woebken, D., Fuchs, B. M., Kuypers, M. M. M, and Aman, R.: Potential interactions of particle-associated
1039 anammox bacteria with bacterial and archaeal partners in the Namibian upwelling system, Appl.
1040 Environ. Microbiol., 73, 4648-4657, 2007.
1041 Wörmer, L., Lipp, J. S., Schröder, J. M., and Hinrichs, K.-U.: Application of two new LC-ESI-MS
1042 methods for improved detection of intact polar lipids (IPLs) in environmental samples, Org. Geochem.
1043 59, 10–21, 2013.
1044 Wright, J. J., Konwar, K. M., and Hallam, S. J: Microbial ecology of expanding oxygen minimum zones,
1045 Nat. Rev. Microbiol. 10, 381-394, 2012.
1046 Xie, S., Liu, X.-L., Schubotz, F., Wakeham, S. G., and Hinrichs K.-U.: Distribution of glcerol ether lipids
1047 in the oxygen minimum zone of the Easter Tropical North Pacific Ocean, Org. Geochem. 71, 60–71,
1048 2014.
1049 Yao, M., Elling, F. J., Jones, C., Nomosatryo, S., Long, C. P., Crowe, S. A., Antoniewicz, M. R., Hinrichs,

K.-U., and Maresca, J. A.: Heterotrophic bacteria from an extremely phosphate-poor lake have conditionally reduced phosphorus demand and utilize diverse sources of phosphorus, Environ. Microbiol. 18, 656–667, 2015.

Zavaleta-Pastor, M., Sohlenkamp, C., Gao, J. L., Guan, Z., Zaheer, R., Finan, T. M., Raetz, C. R. H., López-Lara, I. M., and Geiger, O.: Sinorhizobium meliloti phospholipase C required for lipid remodeling during phosphorus limitation, Proc. Natl. Acad. Sci. USA, 107, 302–307, 2010.

Zhang, Y.-M., and Rock, C. O.: Membrane lipid homeostasis in bacteria, Nat. Rev. Microbiol., 6, 222–233, 2008.

Zhu, C., Wakeham, S. G., Elling, F. J., Basse, A., Mollenhauer, G., Versteegh, G. J. M., Könneke, M., and Hinrichs, K.-U.: Stratification of archaeal membrane lipids in the ocean and implications for adaptation and chemotaxonomy of planktonic archaea, Environ. Microbiol. 18, 4324-4336, 2016.

Tables

Table 1. Spearman Rank Order Correlation coefficients (r) for data combined from all four stations. Only significant correlations, where $p < 0.05$ (highly significant $p < 0.001$, in bold), are presented.

	Glycolipids						Aminolipids				Phospholipids					
	% GL	% 1G	% 2G	% SQ	GL:PL	SQ:PG	% AL	% DGTS	AL:PL	DGTS:PC	% PL	% PC	% PG	% PE	% PME	% PDME
Depth	-0.32		**-0.7**	**-0.67**	-0.41	**-0.76**										
Fluorescence			**0.63**	**0.67**		**0.65**										
POC			**0.61**	**0.6**		**0.6**										
TN			**0.66**	**0.62**		**0.63**										
Oxygen	**0.57**	0.3	**0.48**	0.35	**0.55**	**0.58**			0.36		**-0.49**		-0.38	-0.33	-0.46	-0.52
Temperature	0.3		**0.52**	**0.63**	0.39	**0.69**										
Chl a	0.35		**0.72**	**0.71**	0.42	0.78										-0.33
Phosphate			**-0.62**	**-0.53**	-0.4	**-0.56**										0.36
Nitrate			**-0.53**	**-0.49**		-0.38										
Nitrite		-0.33													0.3	
Ammonium							0.41	0.42	0.35	0.4						
N:P			-0.3	-0.32									-0.36			

Abbreviations: GL – glycolipids, 1G – monoglycosyl, 2G – diglycosyl, SQ – sulfoquinovosyl, PL – phospholipids, AL – aminolipids, DGTS – diacylglyceryl trimethyl homoserine, PC – phosphatidyl choline, PG – phosphatidyl glycerol, PE – phosphatidyl ethanolamine, PME – phosphatidyl methyl-ethanolamine, PDME – phosphatidyl dimethyl-ethanolamine

Figures

Figure 1. a) Map of ETNP with R/V *Seward Johnson* (November 2007) cruise sampling stations investigated in this study.

Figure 2. Depth profiles of (a) oxygen and temperature, (b) chlorophyll-α and transmissivity, (c) particulate organic matter (POC) and C:N, (d) intact polar lipid (IPL) to POC ratio and IPL concentration, and (e) absolute cell abundance and relative proportions of archaeal cells (data from Podlaska et al. (2012)). C:N (SPM) is total carbon over total nitrogen of the solid phase collected by water filtration. Note that C:N, POC and IPL/POC are only analyzed for <53 μm particle fraction. Also depicted are the different geochemical zones in the water column.

Figure 3. Depth profiles of (a) nitrate, nitrite, and ammonium, (b) phosphate and N:P, (c) total non-archaeal (non-isoprenoidal) phospholipids, glycolipids and (d) aminolipids shown as percent of total intact polar lipids and ratios of non-phospholipids to phospholipids for DGTS to PC-DAG (e) SQ-DAG to PG-DAG, (e), and 1G-DAG to PE-DAG. Also depicted are the different geochemical zones in the water column.

Figure 4. Relative abundance of (a) major and (b) minor IPLs at sampled depths of stations 1, 2, 5, and 8 in the ETNP. Major IPLs are defined as those comprising more than 10% of total IPLs (minor compounds comprised less than 10%) at more than one depth horizon at the four stations. Also depicted are the different geochemical zones in the water column.

Figure 5. Changes in average carbon atoms (CA) and number of double bond equivalents (DB) of the alkyl side chains of major IPLs detected at stations 1, 2, 5 and 8 in the ETNP.

Figure 6. Nonmetric multidimensional scaling (NMDS) ordination plot assessing the relationship between IPL biomarkers, sampling depths and geochemical parameters in the ETNP (stress=0.125). Squares represent the water depth of each sample and are color-coded according to the defined geochemical zonation. Filled circles stand for lipid distribution of major IPLs and open circles for minor IPLs on the ordination. Vector lines of geochemical parameters are weighted by their p-values with each NMDS axis.

fig01

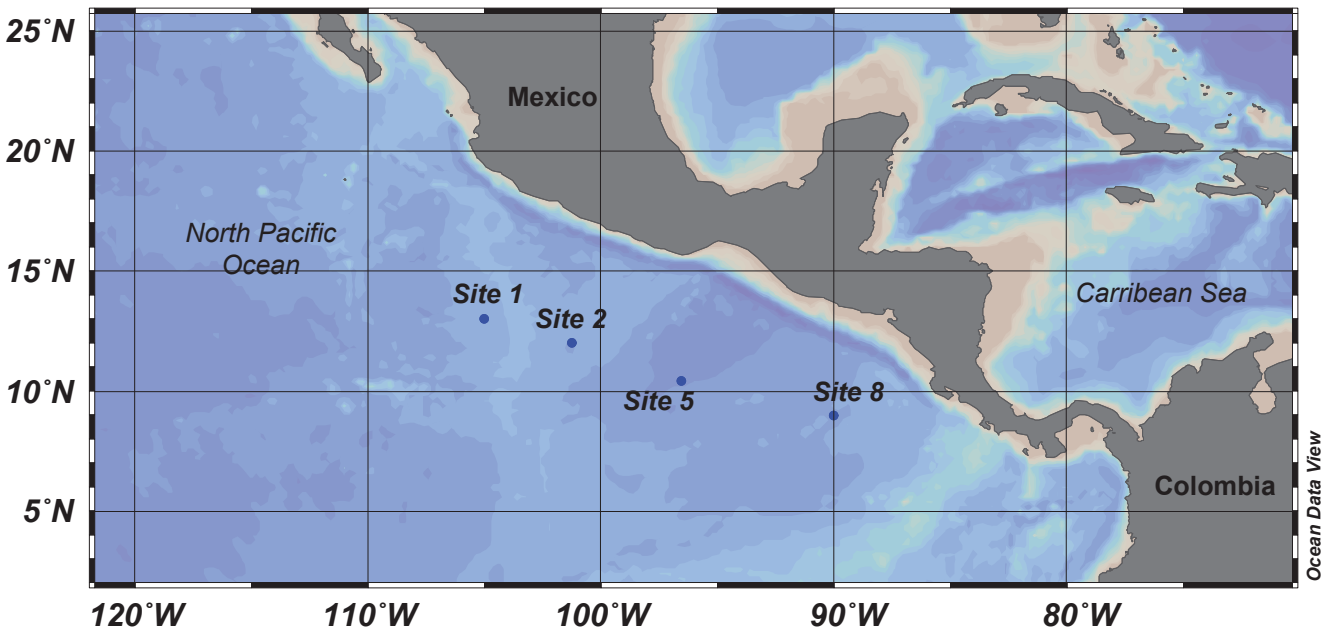
25˚N
20˚N
15˚N
10˚N
5˚N
120˚W
110˚W
100˚W
90˚W
80˚W
Mexico
North Pacific Ocean
Carribean Sea
Colombia
Site 1
Site 2
Site 5
Site 8
Ocean Data View

fig02

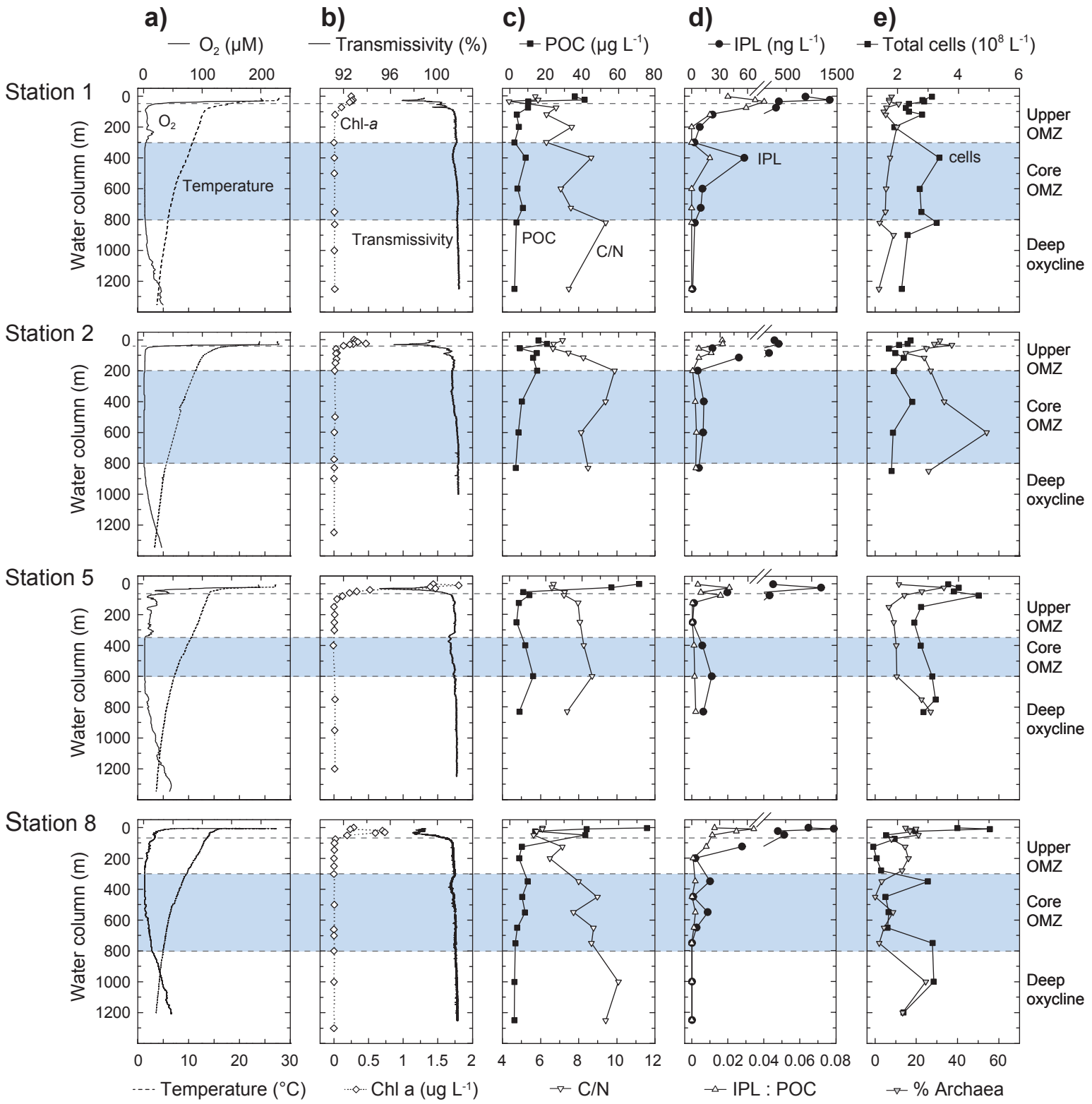
a)
b)
c)
d)
e)
O2 (µM)
Transmissivity (%)
POC (µg L-1)
IPL (ng L-1)
Total cells (10^8 L-1)
Station 1
Station 2
Station 5
Station 8
Water column (m)
O2
Temperature
Chl-a
Transmissivity
POC
C/N
IPL
cells
Upper OMZ
Core OMZ
Deep oxycline
Temperature (°C)
Chl a (ug L-1)
C/N
IPL : POC
% Archaea

fig03

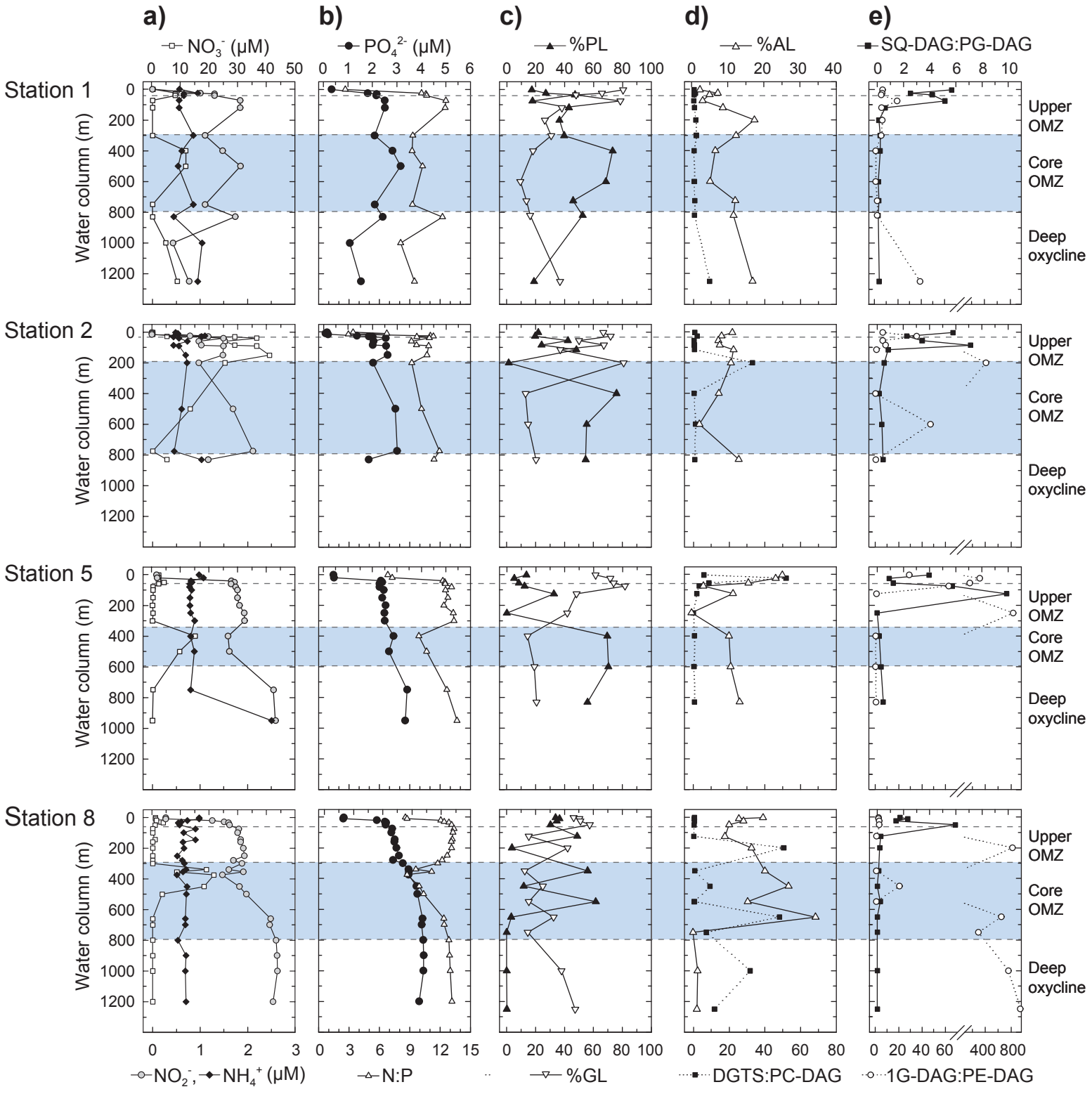

Figure 3

fig04

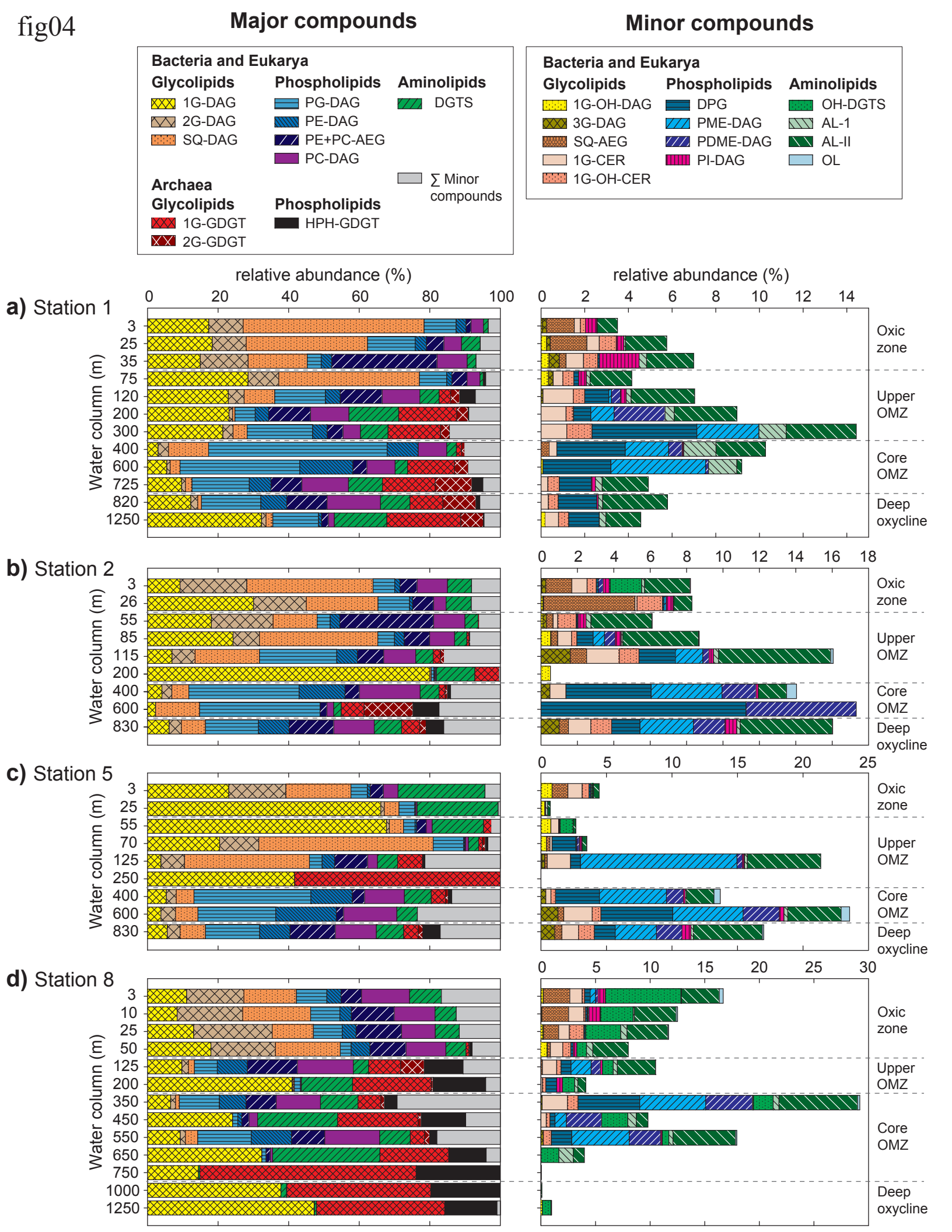
Major compounds
Minor compounds
Bacteria and Eukarya
Glycolipids
1G-DAG
2G-DAG
SQ-DAG
Phospholipids
PG-DAG
PE-DAG
PE+PC-AEG
PC-DAG
Aminolipids
DGTS
∑ Minor compounds
Archaea
Glycolipids
1G-GDGT
2G-GDGT
Phospholipids
HPH-GDGT
Bacteria and Eukarya
Glycolipids
1G-OH-DAG
3G-DAG
SQ-AEG
1G-CER
1G-OH-CER
Phospholipids
DPG
PME-DAG
PDME-DAG
PI-DAG
Aminolipids
OH-DGTS
AL-1
AL-II
OL
relative abundance (%)
relative abundance (%)
a) Station 1
b) Station 2
c) Station 5
d) Station 8
Water column (m)
Oxic zone
Upper OMZ
Core OMZ
Deep oxycline

fig05

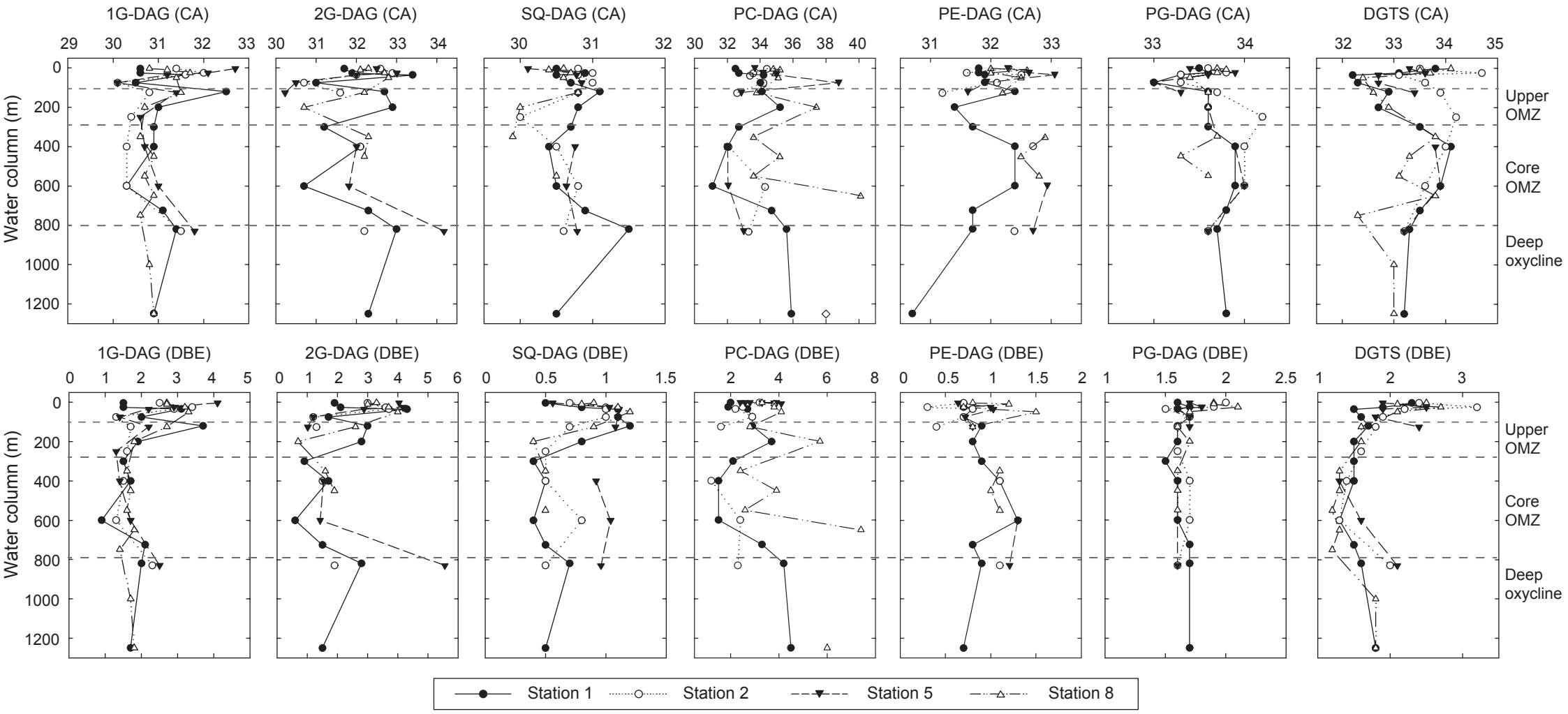
1G-DAG (CA)
2G-DAG (CA)
SQ-DAG (CA)
PC-DAG (CA)
PE-DAG (CA)
PG-DAG (CA)
DGTS (CA)
1G-DAG (DBE)
2G-DAG (DBE)
SQ-DAG (DBE)
PC-DAG (DBE)
PE-DAG (DBE)
PG-DAG (DBE)
DGTS (DBE)
Water column (m)
Upper OMZ
Core OMZ
Deep oxycline
Station 1
Station 2
Station 5
Station 8

fig06

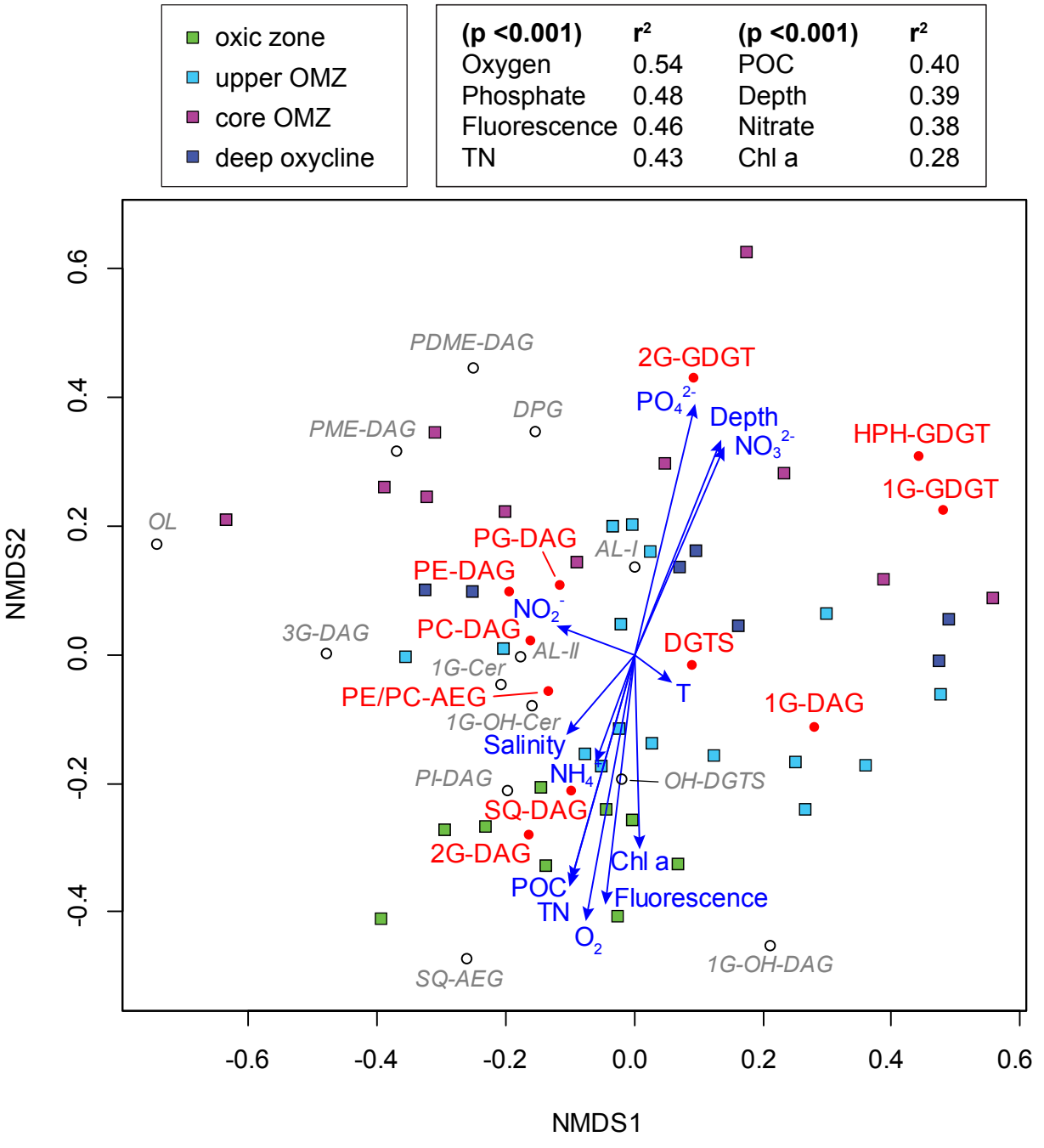
oxic zone
upper OMZ
core OMZ
deep oxycline
(p <0.001) r²
Oxygen 0.54
Phosphate 0.48
Fluorescence 0.46
TN 0.43
(p <0.001) r²
POC 0.40
Depth 0.39
Nitrate 0.38
Chl a 0.28
PDME-DAG
2G-GDGT
PO4 2-
DPG
Depth
NO3 2-
PME-DAG
HPH-GDGT
1G-GDGT
OL
PG-DAG
AL-I
PE-DAG
NO2 -
3G-DAG
PC-DAG
AL-II
DGTS
1G-Cer
T
PE/PC-AEG
1G-DAG
1G-OH-Cer
Salinity
PI-DAG
NH4
OH-DGTS
SQ-DAG
2G-DAG
Chl a
POC
TN
Fluorescence
O2
SQ-AEG
1G-OH-DAG
NMDS1
NMDS2
-0.6
-0.4
-0.2
0.0
0.2
0.4
0.6